Propagation Modeling for Wireless Sensor Networks

Claude Oestges

Université catholique de Louvain

Louvain-la-Neuve, Belgium

Acknowledgments

- Some of these slides include contributions from
  - Mischa Dohler (CCTC)
  - Farshad Keshmiri (UCL)
  - Stéphane van Roy (UCL-ULB)
  - …

Propagation Modeling for WSNs

- **Introduction to propagation and channel modeling**
  - Path-loss
  - Shadowing
  - Fading
  - Frequency selectivity
  - Spatial dispersion
  - Modeling approaches

Propagation Modeling for WSNs (2)

- **Particularities of WSNs**
  - Transmission media
  - Virtual MIMO
  - Relay channels

- **Examples**
  - Environmental WSNs (in forested areas)
  - Body area networks

Part I
Introduction to Propagation and Channel Modeling

Propagation Modeling

- **Usually, channel modelling is made of three parts**
  - **Path-loss** determines the average (over local space and time) power received for a given Tx-Rx range
  - **Shadowing** is added to the path-loss to account for local large-scale effects (obstruction, etc.)
  - **Fading** represents the short-term variations of the received power and is caused by multi-path propagation
- **This classification is slightly canonical**
  - But it is also extremely useful, as each effect impacts (or is solved by) different signal processing/networking/routing algorithms

Path Loss

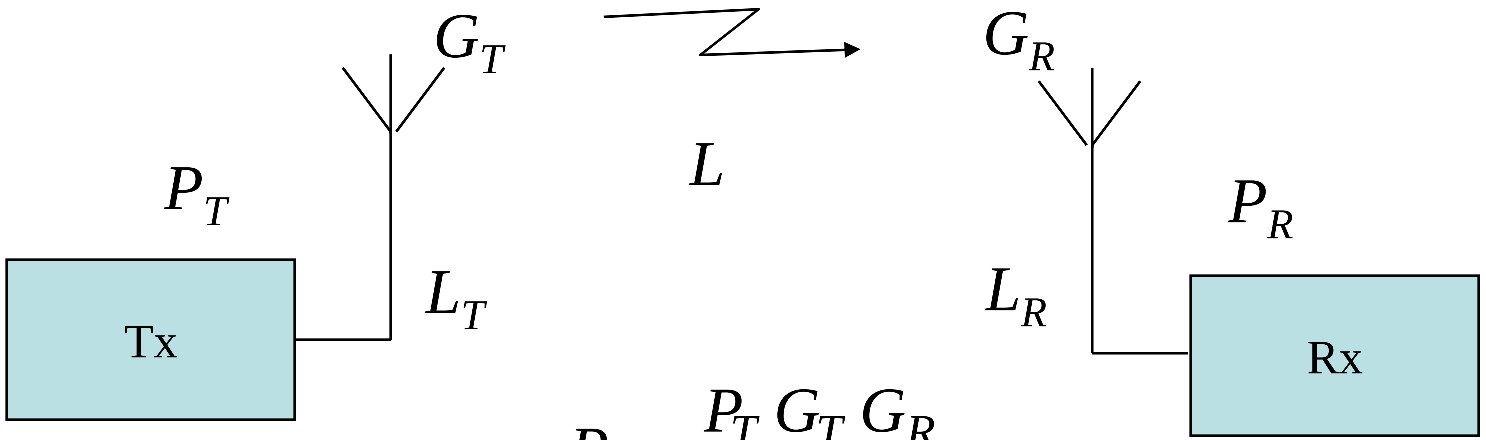

$$P_R = \frac{P_T\, G_T\, G_R}{L\, L_T\, L_R}$$

- P_R is the power at the receive (Rx) node
- P_T is the power at the transmit (Tx) node
- G_T is the gain of Tx antenna (dBi)
- G_R is the gain of Rx antenna (dBi)
- L is the path loss
- $L_{T,R}$ are the cable losses (Tx, Rx)

Path Loss in Free Space

- We can easily express that

$$\frac{P_R}{P_T} = G_R G_T \left(\frac{\lambda}{4\pi r} \right)^2$$

- **The free space path loss becomes**

$$\boxed{L = \frac{P_T G_T G_R}{P_R} = \left(\frac{4\pi r}{\lambda} \right)^2}$$

  - Path loss exponent = 2
  - $P_T G_T$ = transmit EIRP (effective isotropic radiated power)

Plane Earth Path Loss

- WSN environment is not governed by free space losses owing to the presence of the ground

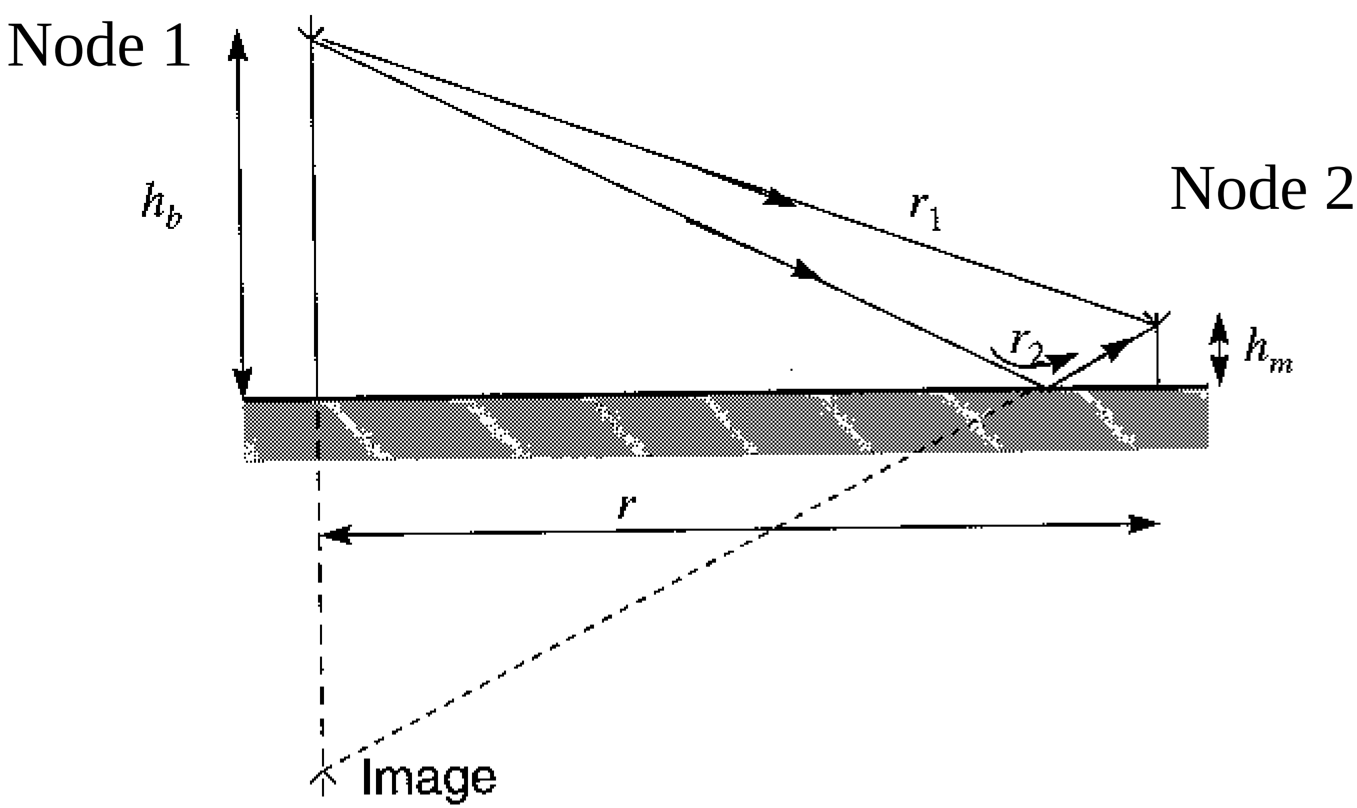

Plane Earth Path Loss (2)

- It can be shown that

$$P_R \cong P_T \left(\frac{h_m h_b}{r^2} \right)^2$$

  - The path loss is
    - increasing with the distance by 40 dB/decade (path-loss exponent = 4)
    - decreasing with antenna heights
  - This is still not an accurate model of propagation; in general,

$$L(dB) = 10 n \log r$$

  - In general, $n \in [1, 4]$

Canyons (waveguiding)

Deep shadowing (obstruction)

Plane Earth Path Loss + Clutter Factor

$$L = \text{Plane Earth Loss} + \text{Clutter Factor}$$
$$= 40\log R + 20\log f_c - 20\log h_b + L_m$$

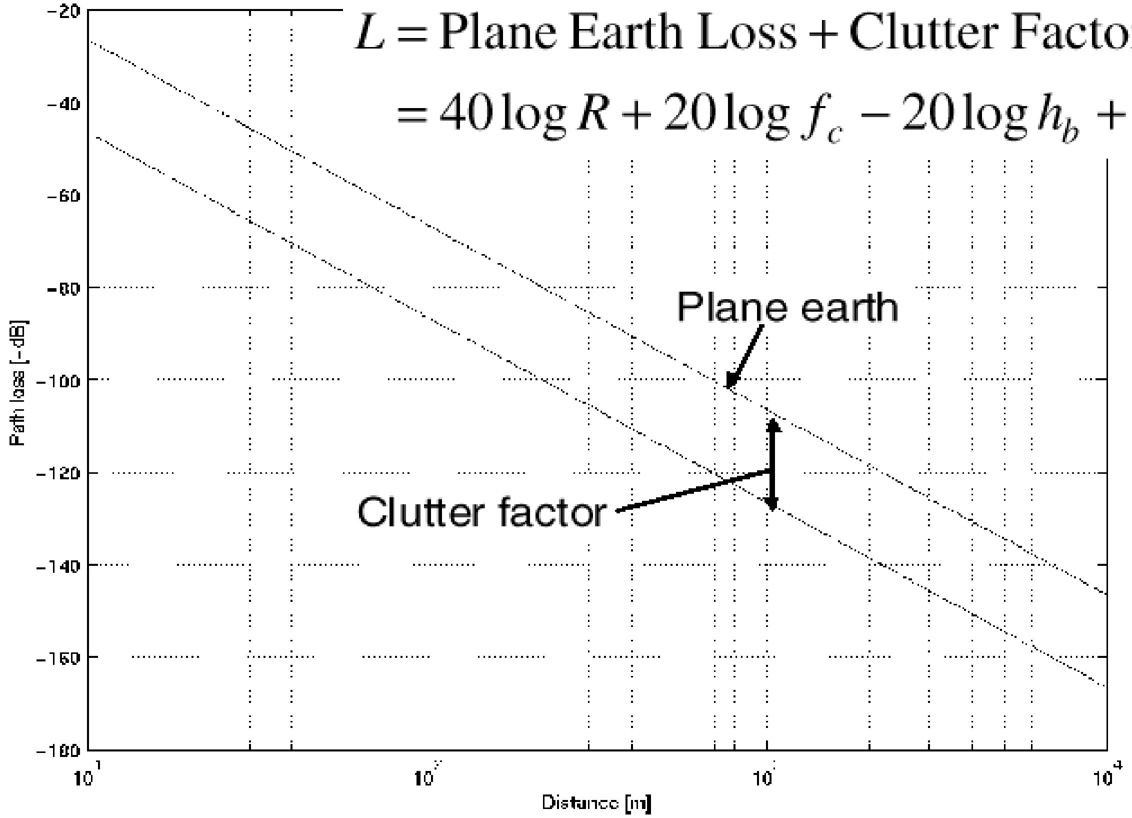

J. Egli, “Radiowave propagation above 40 Mc over irregular terrain”, Proc. IRE, pp. 1383-1391, 1957.
G. Delisle, J. Lefèvre, M. Lecours, J. Chouinard, ‘Propagation loss prediction : a comparative study with application to the mobile radio channel”, IEEE Trans. Veh. Techn., vol.26, n)4, pp. 295-308, 1985.

About Empirical Models

- **Limitations of empirical path-loss models**
  - They can only be used over parameter ranges included in the original measurement set
  - Environment must be classified subjectively according categories, which may be different in different countries.
  - They provide no physical insight into the mechanisms by which propagation occurs

- **Advantages of empirical models**
  - They are very simple and offer a good approximation of the average loss

Shadowing

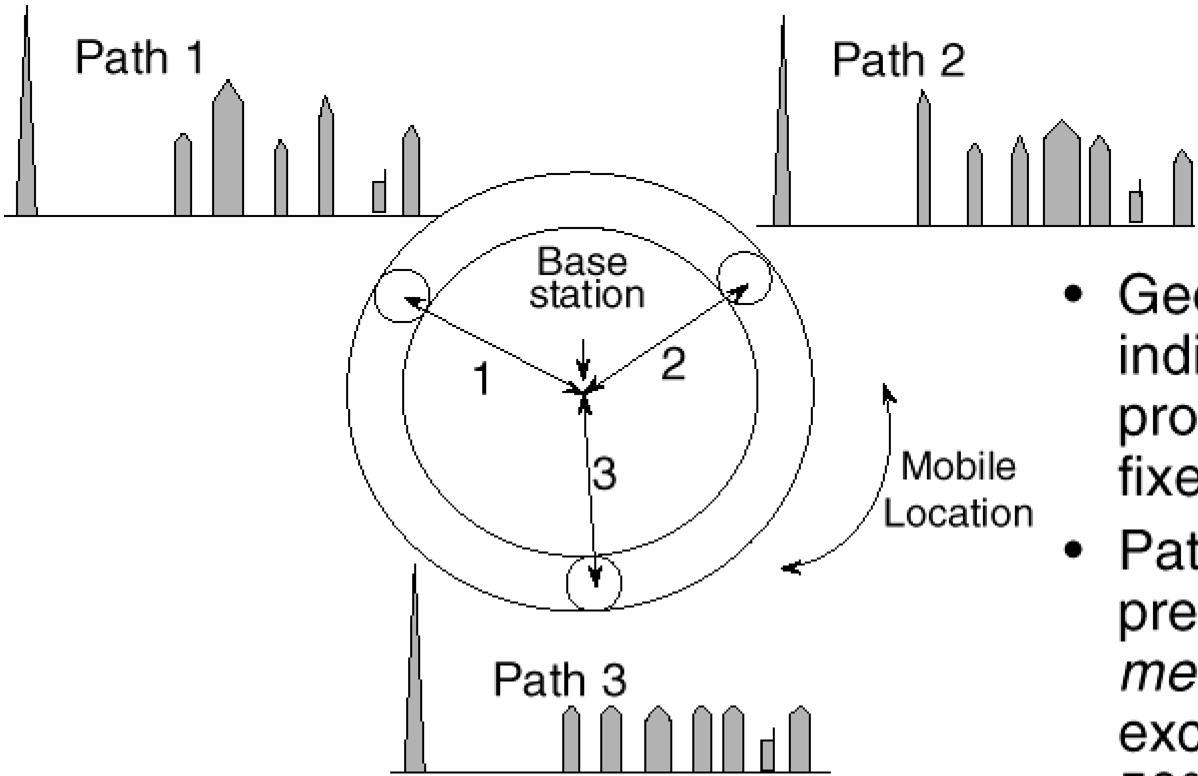

- Geometry of individual path profiles varies at fixed distance
- Path loss models predict the *median* level, exceeded at 50% of locations

Shadowing (2)

- Typical variation of shadowing with Rx node position, at a fixed distance of another (Tx) node

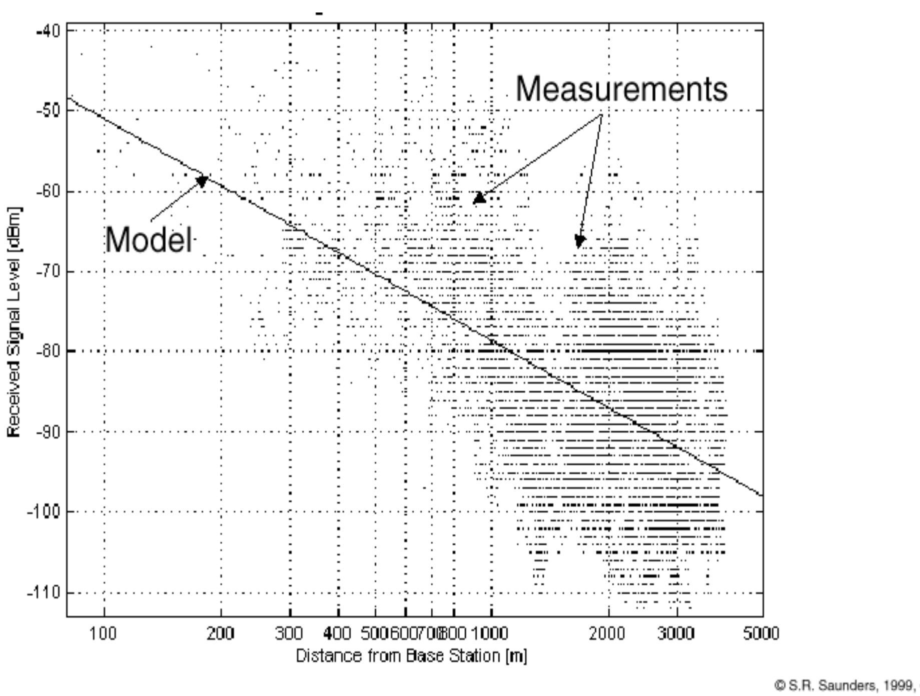

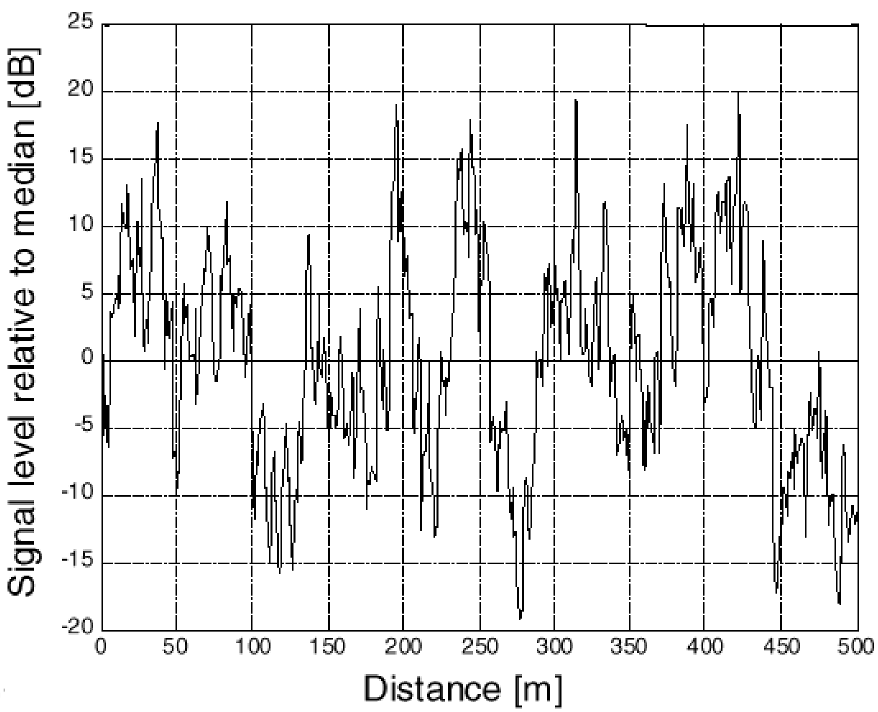

$$L_S(dB) = L + \Xi_{dB} = L + 20\log_{10}\Xi$$

Shadowing (3)

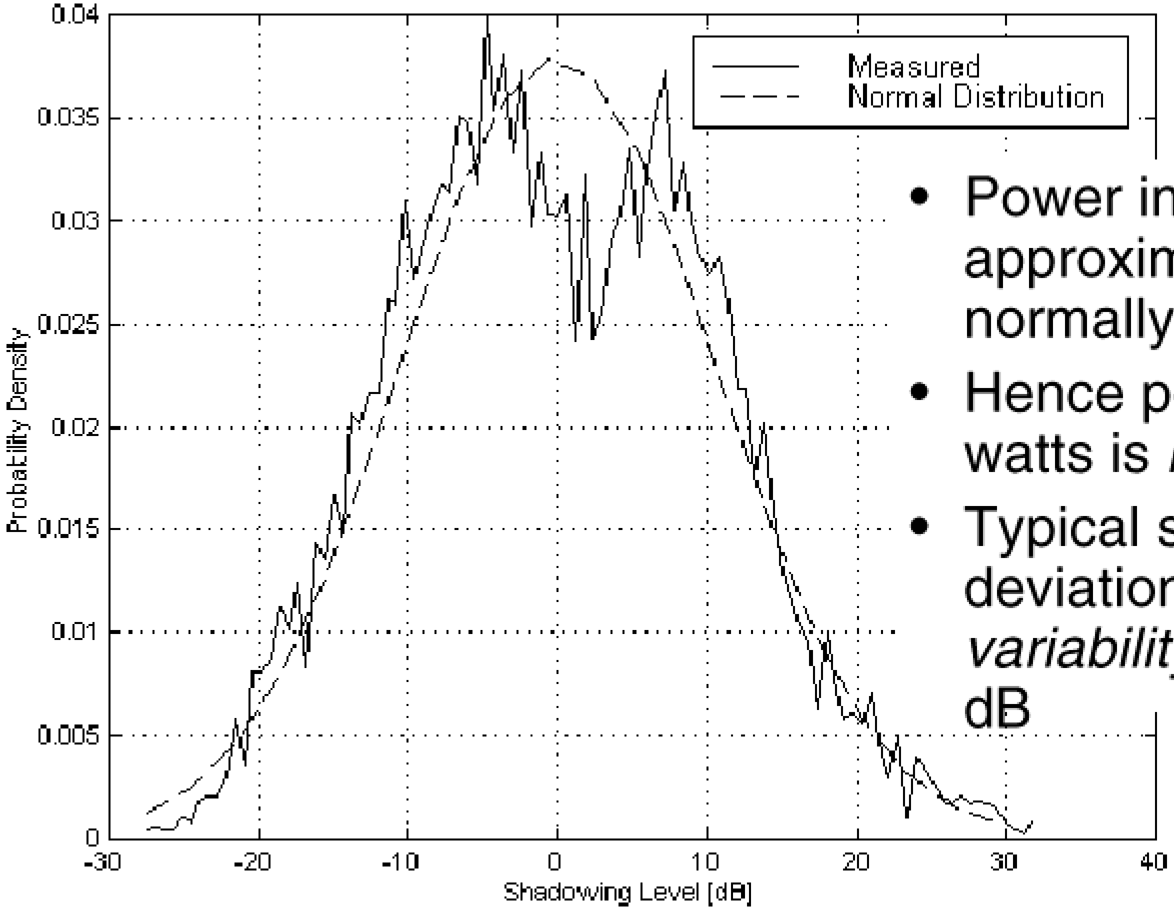

- Power in dB is approximately normally distributed
- Hence power in watts is *lognormal*
- Typical standard deviation (*location variability*) of 5-12 dB

.R. Saunders, 1999,

Fading

- On top of path loss and shadowing, significant variations can be observed over time, e.g. as a node moves over a few wavelength

⇒ (Fast) fading

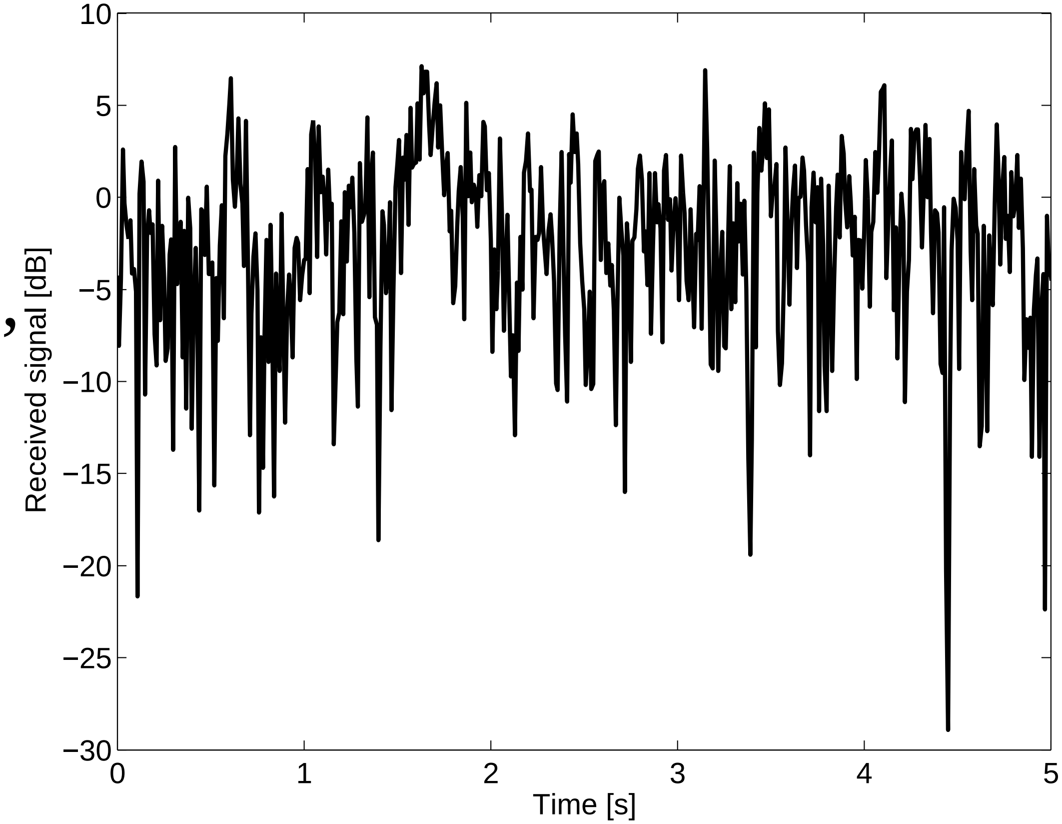

Fading (2)

- **Several scenarios**
  - Mobile Sensor/Sink (MS) to Fixed Sensor/Sink (FS)
  - Mobile Sensor to Mobile Sensor/Sink (MS-MS)
  - Fixed Sensor to Fixed Sensor/Sink (FS-FS)
  - Any combination in multi-hop scenarios
- **First-order statistics**
  - Possibly similar for MS-FS and MS-MS but certainly very different for FS-FS
- **Second-order statistics**
  - Different for each case

Putting It All Together

- **The received signal is written as**

$$y(t) = \underbrace{10^{G_R/20}}_{Rx} \; \underbrace{10^{L/20}}_{path-loss} \cdot \underbrace{\Xi(t)}_{shadowing} \cdot \underbrace{h(t)}_{fading} \cdot \underbrace{10^{P_T G_T/20} c(t)}_{Tx\ EIRP} + \underbrace{n(t)}_{noise}$$

  - For a given Tx-Rx distance, path-loss is fixed
  - Over a local area or over not too long time periods, shadowing is also fixed $\Rightarrow \Xi(t) = \Xi$
  - Hence, the average power is given in dB by

$$P_T G_T + G_R - (L + \Xi_{dB}) \Rightarrow \mathcal{E}\{\,|h|^2\,\} = 1$$

Putting It All Together

- **The received signal is written as**

$$y(t) = \underbrace{10^{G_R/20}}_{Rx} \; \underbrace{10^{L/20}}_{path-loss} \cdot \underbrace{\Xi}_{shadowing} \cdot \underbrace{h(t)}_{fading} \; \underbrace{\cdot 10^{P_T G_T/20} c(t)}_{Tx\ EIRP} + \underbrace{n(t)}_{noise}$$

$$\boxed{E_S}$$

- – For a given Tx-Rx distance, path-loss is fixed
- – Over a local area or over not too long time periods, shadowing is also fixed $\Rightarrow \Xi(t) = \Xi$
- – Hence, the average power is given in dB by

$$P_T G_T + G_R - (L + \Xi_{dB}) \Rightarrow \mathcal{E}\{\,|h|^2\,\} = 1$$

- – E_S is the average received symbol energy (~ SNR)

Putting It All Together (2)

- **The received signal is written as**

$$y(t) = \underbrace{10^{G_R/20}}_{Rx} \underbrace{10^{L/20}}_{path-loss} \cdot \underbrace{\Xi(t)}_{shadowing} \cdot \underbrace{h(t)}_{fading} \underbrace{\cdot 10^{P_T G_T/20} c(t)}_{Tx\ EIRP} + \underbrace{n(t)}_{noise}$$

$$\boxed{E_S}$$

– For a given Tx-Rx distance, path-loss is fixed

– If one considers long-term variations/motions, Ξ is not fixed anymore but slowly varying, yet its average energy is one

– In any case, $\mathcal{E}\{|h|^2\} = 1$ (and same for Ξ)

– E_S is the average received symbol energy (~ SNR)

Multipaths

- Signal propagates from Tx to Rx via various paths

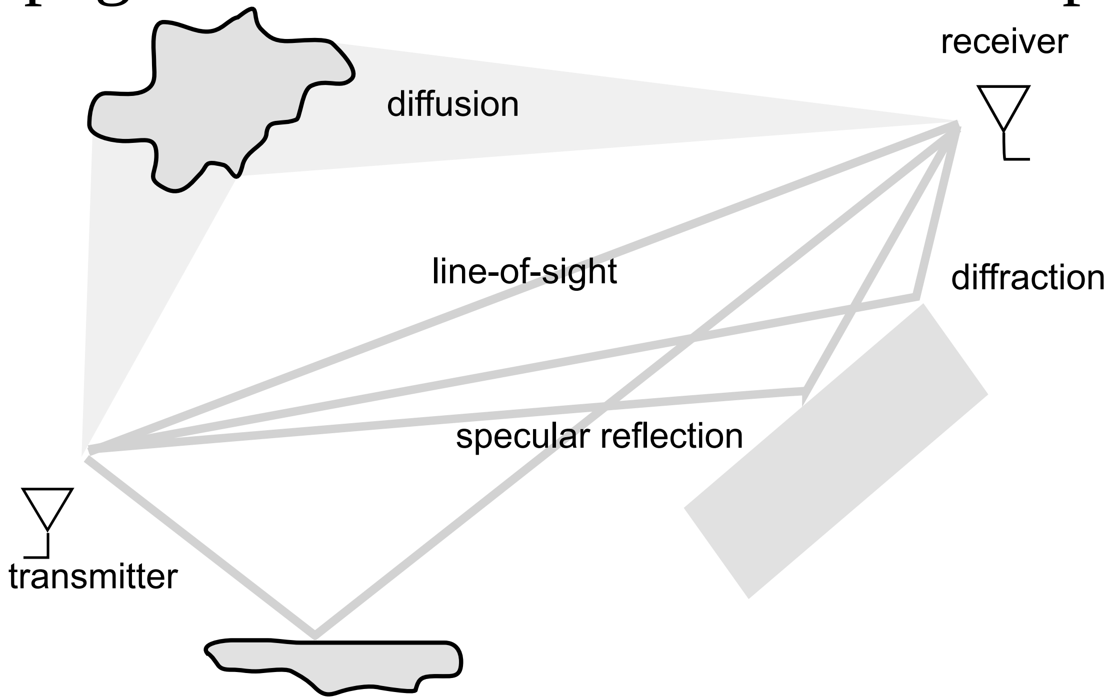

  - The channel is represented by a stochastic function *h*
  - Because path loss is removed, $\mathcal{E}\{\,|h|^2\,\} = 1$

Flat Fading for MS-FS Channels

- Assume that the n_s paths constituting the channel arrive *at the same time*, i.e. during the same symbol interval
  - NB: we denote by *h* the global chain filter

$$y(t) = \sqrt{E_s}\, h(t) c(t) + n(t)$$

Doppler shift $\Delta\omega_k$

$$h(t) = \sum_{k=0}^{n_s-1} h_k(t) = \sum_{k=0}^{n_s-1} \alpha_k \; e^{j\phi_k} \exp\left[-j \frac{2\pi}{\lambda} \cos(\gamma - \vartheta_k) \sin\psi_k \; v \, t \right]$$

  - where γ is the direction of motion in the horizontal plane, ϑ is the azimuth angle of arrival and ψ is the elevation angle of arrival
  - Rayleigh/Ricean fading
  - In general, each path itself is the sum of clustered interfering paths and scatterers may move as well

Flat Fading for MS-FS Channels

- Assume that the n_s paths constituting the channel arrive *at the same time*, i.e. during the same symbol interval
  - NB: we denote by *h* the global chain filter

$$y(t) = \sqrt{E_s}\, h(t) c(t) + n(t)$$

Doppler shift $\Delta\omega_k$

$$h(t) = \sum_{k=0}^{n_s-1} h_k(t) = \sum_{k=0}^{n_s-1} \alpha_k \underline{(t)}\, e^{j\phi_k \underline{(t)}} \exp\left[-j \frac{2\pi}{\lambda} \cos(\gamma - \vartheta_k) \sin\psi_k \; v\, t \right]$$

  - where γ is the direction of motion in the horizontal plane, ϑ is the azimuth angle of arrival and ψ is the elevation angle of arrival
  - Rayleigh/Ricean fading
  - In general, each path itself is the sum of clustered interfering paths and scatterers may move as well

Frequency Selective Fading

- If the n_s paths constituting the channel arrive during different symbol intervals (in the delay domain)

$$\begin{aligned} \mathsf{r}(t) &= \mathsf{h}(t,\tau) \star c(t) + \mathsf{n}(t) \\ &= \int_0^{\tau_{max}} \mathsf{h}(t,\tau) c(t-\tau) d\tau + \mathsf{n}(t) \\ &= \sum_{l=-\infty}^{\infty} \sqrt{E_s} c_l \mathsf{h}_t[t - lT] + \mathsf{n}(t). \end{aligned}$$

$$\boxed{\begin{aligned} h(t,\tau) &= \sum_{k=0}^{n_s-1} h_k(t)\delta(\tau-\tau_k) \\ h_k(t) &= \alpha_k(t)\, e^{j\phi_k(t)} \exp[-j\,\Delta\omega_k t] \exp[-j\,\omega_0 \tau_k] \end{aligned}}$$

Each tap is frequency flat

Frequency Flat vs. Frequency Selective

- **Frequency flat channels** (or narrowand channels)
  - The definition depends on the propagation channel but also on the system bandwidth (which needs to be « small »)
  - The transfer function (Fourier transform along the delay dimension τ) is flat, hence the name
  - We will characterize the statistics of the amplitude $s = |h(t)|$, including fade dynamics
  - Note also that

$$\boxed{h(t) = \int_0^{\tau_{max}} h(t,\tau)\, d\tau}$$

Frequency Flat vs. Frequency Selective (2)

- **Frequency selective channels** (or wideband)
  - Each tap is a frequency flat channel (characterized as above), but the global transfer function is not flat anymore
  - Consequence: Inter-symbol interference (ISI)

Flat Fading for MS-MS Channels

- Generalize the previous representation for mobile Tx and Rx

$$h(t)=\sum_{k=0}^{n_s-1} h_k(t)=\sum_{k=0}^{n_s-1}\alpha_k\; e^{j\phi_k}\exp\left[-j\frac{2\pi}{\lambda}\cos(\gamma_1-\vartheta_{k,1})\sin\psi_{k,1}\;v_1\;t\right]$$

$$\cdot\exp\left[-j\frac{2\pi}{\lambda}\cos(\gamma_2-\vartheta_{k,2})\sin\psi_{k,2}\;v_2\;t\right]$$

  – The fading amplitude will be Rayleigh/Ricean distributed

Rayleigh Fading

- Statistics of channel amplitude
  - Assume each path has the same average energy and apply the central limit theorem

$\Rightarrow$ *h* is a circularly zero mean complex variable

$\Rightarrow$ *s* is Rayleigh distributed

$$p_s(s) = \frac{s}{\sigma_s^2} \exp\left(-\frac{s^2}{2\sigma_s^2}\right) \Rightarrow \begin{array}{rcl} \mathcal{E}\{s\} & = & \sigma_s\sqrt{\frac{\pi}{2}} \\ \mathcal{E}\{s^2\} & = & 2\sigma_s^2 = 1, \end{array}$$

by definition of fading

$\Rightarrow$ the phase of *h* is uniform over $[0, 2\pi]$

Rayleigh Fading (2)

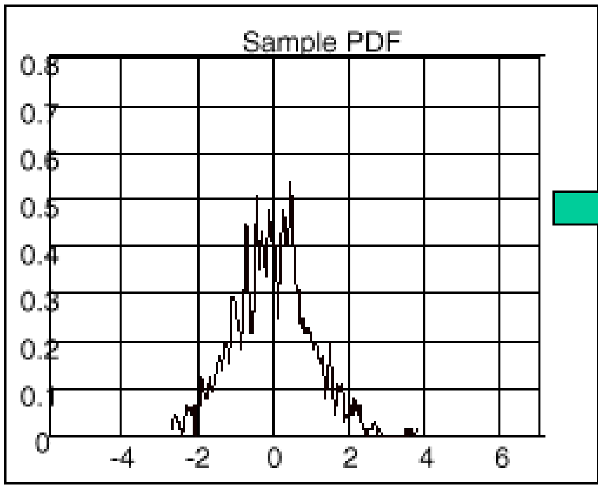

Imaginary (Quadrature) part

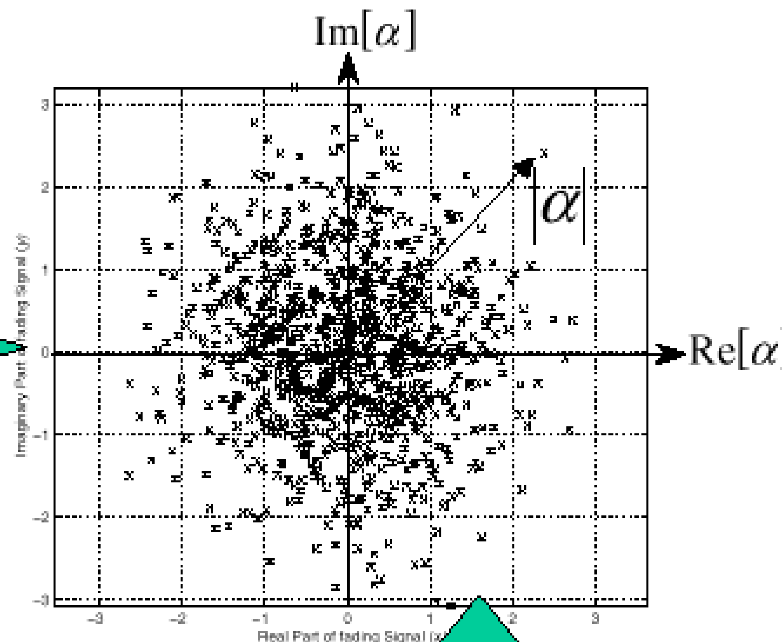

Complex baseband signal (Rice representation)

Real (In-phase) part

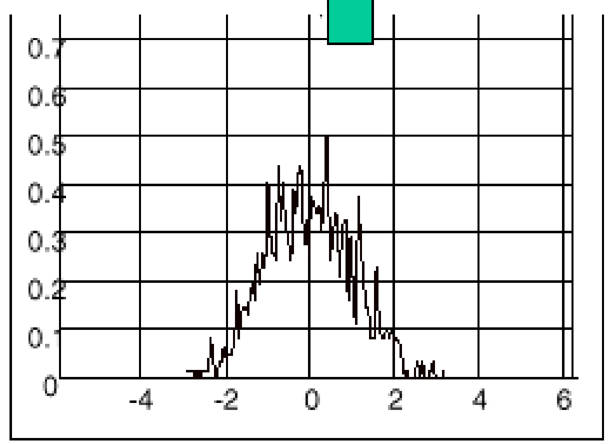

Ricean Fading

- What if one or more paths are coherent ? (i.e. do not vary over time !)
  - In that case, we may write

$$h = \bar{h} + \tilde{h} = \sqrt{\frac{K}{K+1}} e^{j\phi_c} + \sqrt{\frac{1}{K+1}} \frac{\tilde{h}}{\sqrt{2}\sigma_s}$$

where the K-factor K is defined by $K = \frac{|\bar{h}|^2}{2\sigma_s^2}$

$\Rightarrow$ $s' = |h|$ is a Ricean variable variable

$$p'_s(s') = \frac{2s'K}{|\bar{h}|^2} \exp\left[-K\left(\frac{s'^2}{|\bar{h}|^2} + 1\right)\right] I_0\left(\frac{2s'K}{|\bar{h}|}\right)$$

Ricean Fading

- What i… …e. do not vary o…
  – In th…

h…

where …

$\Rightarrow$ s' = …

$$p'_s(\ldots \frac{\ldots}{|\bar{h}|} \ldots \Big[\ldots \Big(\frac{\ldots}{|\bar{h}|} \ldots \Big) \Big] \ldots \Big(\frac{2s'K}{|\bar{h}|} \Big)$$

This is not LOS vs. NLOS !

The coherent part itself is the sum of a LOS and a scattered contribution

Time Correlation for MS-FS Rayleigh Channels

- Assuming that $h(t)$ is wide-sense stationary, we define the time correlation as

$$R_h(\Delta t) = E\{h(t)h^*(t+\Delta t)\} = \sum_k |\alpha_k|^2 e^{j\Delta\omega_k \Delta t} + \underbrace{\sum_{k,k'} \alpha_k \alpha_{k'} \ldots}_{=0}$$

if all paths are i.i.d.

- If all paths are i.i.d. we can replace the sum by an integral, taking the limit for $n_s \to \infty$

$$R_h(\Delta t) = \iint_{\psi,\vartheta} e^{j\frac{2\pi}{\lambda}\cos(\gamma-\vartheta)\sin\psi\, v\, \Delta t} p_\vartheta(\vartheta)\, p_\psi(\psi)\, d\vartheta\, d\psi$$

Time Correlation for MS-FS Rayleigh Channels (2)

- The temporal correlation is related to the distribution of azimuth and elevation (assuming equal paths)
- Considering the case $\begin{cases} p_\vartheta(\vartheta) = 1/2\pi \\ p_\psi(\psi) = \delta(\psi - \pi/2) \end{cases}$

$$\Rightarrow \boxed{R_h(\Delta t) = J_0\left(\frac{2\pi}{\lambda} v\,\Delta t\right) = J_0(\nu_m\,\Delta t)}$$

where $\nu_m = 2\pi/\lambda\, v$

  - The fading signal is thus not white, but the more distant in time the samples, the less correlated
  - If there is a LOS, a constant term appears in the correlation

Time Correlation for MS-FS Rayleigh Channels (3)

- Correlation between fields at two points separated in **time**

$$R_h(\Delta t) = J_0\left(\frac{2\pi}{\lambda} v \, \Delta t\right)$$

Coherence Time: $T_C \approx \dfrac{9}{16\pi \nu_m}$

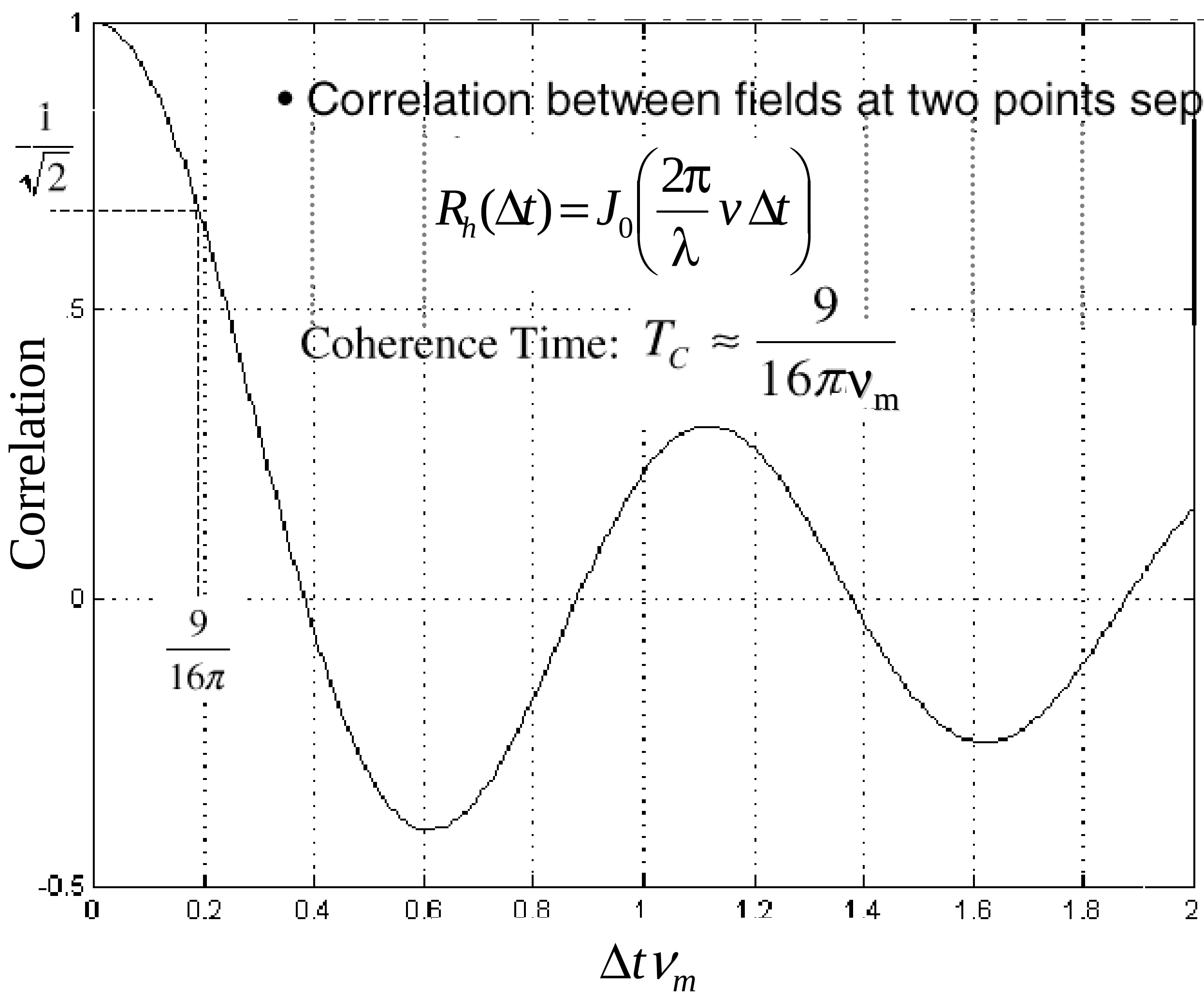

...nders, 1999,

Doppler Spectrum for MS-FS Rayleigh Channels

- The Doppler spectrum is the Fourier transform of the temporal correlation
- For the considered case

$$\mathcal{S}(\nu) = \frac{3}{2\pi\nu_m\sqrt{1-\frac{\nu^2}{\nu_m^2}}} \quad \text{for} \quad |\nu| < \nu_m$$

$$= 0 \text{ for } |\nu| \geq \nu_m$$

where $\nu_m = 2\pi/\lambda\ v = 2\pi\ f_0 v/c$ is the maximum Doppler shift proportional to the sensor's speed and the carrier frequency

– If there is a LOS, a delta function appears in the spectrum

Time Correlation for MS-MS Rayleigh Channels

- By generalization of the MS-FS case, we have for isotropic Rayleigh scattering [Patel, 2005]

$$\boxed{\begin{aligned} R_h(\Delta t) &= J_0\left(\frac{2\pi}{\lambda} v_1 \, \Delta t\right) \cdot J_0\left(\frac{2\pi}{\lambda} v_2 \, \Delta t\right) \\ &= J_0\left(\frac{2\pi}{\lambda} v_1 \, \Delta t\right) \cdot J_0\left(\frac{2\pi}{\lambda} a v_1 \, \Delta t\right) \end{aligned}}$$

where $a = v_2/v_1$

- If there is a LOS, a constant term appears in the correlation
- Nothing to do with double-Rayleigh fading (keyhole in MIMO)

Doppler Spectrum for MS-MS Rayleigh Channels

- Taking the Fourier transform of the previous expression yields the Doppler spectrum [Patel, 2005]

$$\boxed{S(\nu) = \frac{1}{\pi^2 \nu_{m,1} \sqrt{a}} K\left[\frac{1+a}{2\sqrt{a}} \sqrt{1 - \left(\frac{\nu}{(1+a)\nu_{m,1}} \right)} \right]}$$

where $K[.]$ is the complete elliptic integral of the first kind

- If there is a LOS/coherent component, a delta function is added in the spectrum

Doppler Spectrum for FS-FS Channels

- In fixed channels, we have Ricean fading (includes Rayleigh)
  - For high K-factors, the temporal correlation is almost one, as only scatterers are moving, so the channel is not varying a lot

$$h(t) = \sum_{k=0}^{n_s - 1} \alpha_k(t)\, e^{j\phi_k(t)}$$

- The Doppler spectrum can then be very peaky around 0 Hz, but can hardly be estimated analytically

Typical Doppler Spectra

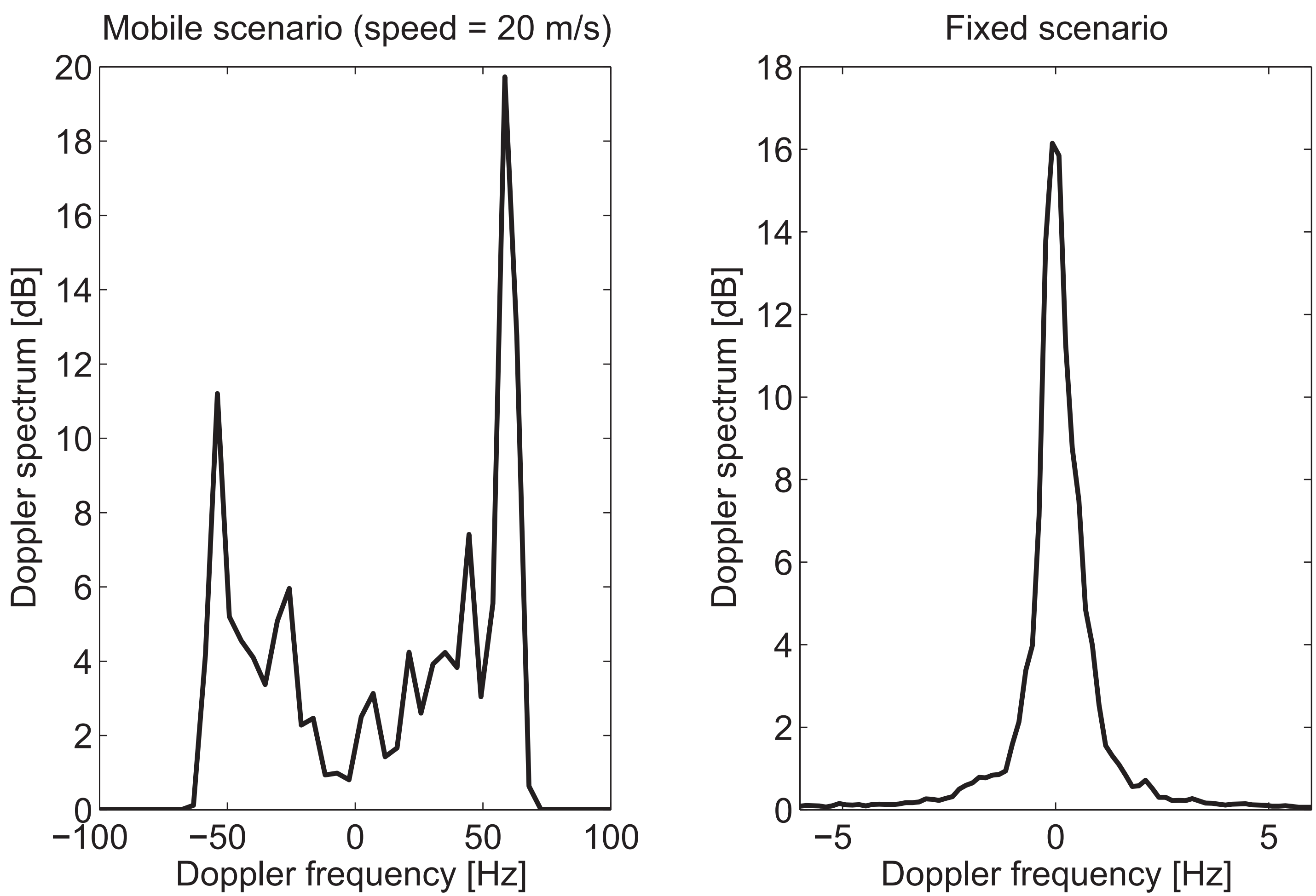

Bi-Dimensional Transfer Functions

- So far, we have dealt with the CIR, but other transfer function can be defined by Fourier transforms

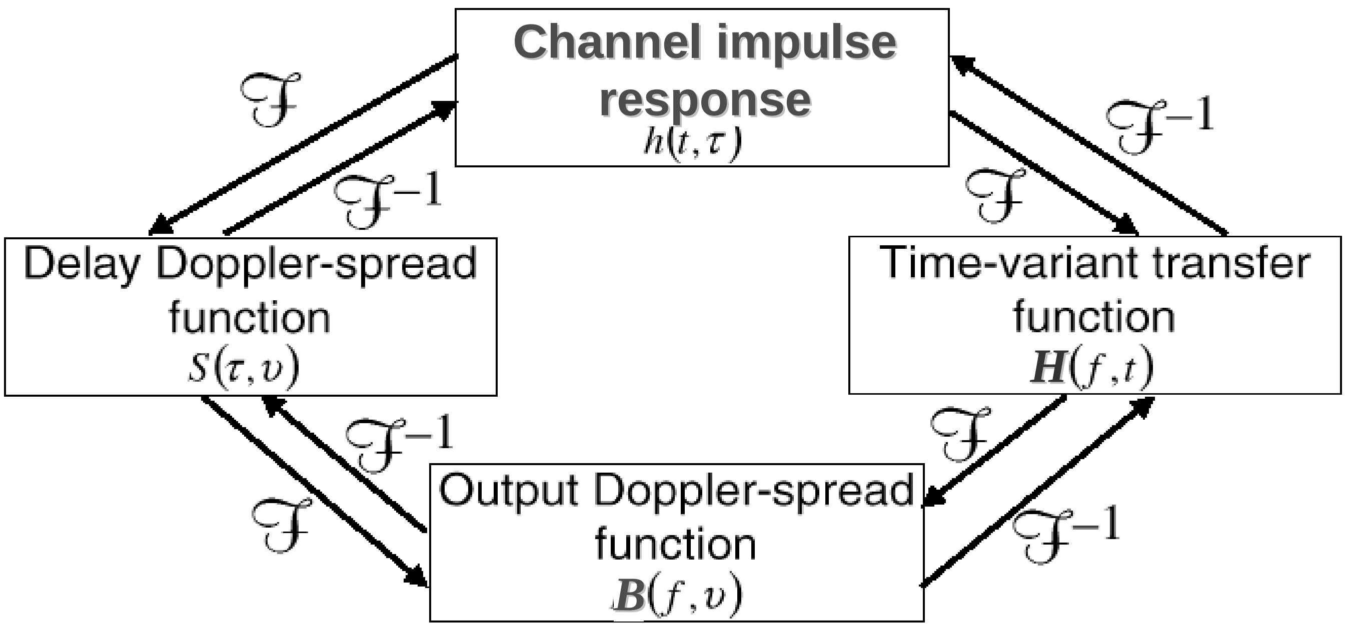

Bi-Dimensional Correlation Functions

- The various transfer functions are random functions
  - Ideally, they should be characterized by joint probability density functions (all orders)
  - But if the channel is complex Gaussian, only the first two orders are required

$$R_h(t, t+\Delta t, \tau, \tau+\Delta\tau) = E\left\{h(t,\tau)h^*(t+\Delta t, \tau+\Delta\tau)\right\}$$

  - We define 3 additional correlation functions

$$R_H(t, t+\Delta t, f, f+\Delta f) \qquad R_S(\nu, \nu+\Delta\nu, \tau, \tau+\Delta\tau)$$

$$R_B(\nu, \nu+\Delta\nu, f, f+\Delta f)$$

WSS-US Channels

- **Wide Sense Stationarity (WSS) assumption**
  - Time correlation functions R_h and R_H only depend on Δt (and not t)

    $\Leftrightarrow$ Signals arriving with different Doppler frequencies are uncorrelated R_B and $R_S \sim \delta(\Delta\nu)$
- **Uncorrelated Scattering (US) assumption**
  - Frequency correlation functions R_B and R_H only depend on Δf

    $\Leftrightarrow$ Signals arriving with different delays are uncorrelated, R_h and $R_S \sim \delta(\Delta\tau)$
- **WSSUS channels**

$$\boxed{R_S(\nu, \nu + \Delta\nu, \tau, \tau + \Delta\tau) = \mathscr{C}_S(\nu, \tau)\delta(\Delta\nu)\delta(\Delta\tau)}$$

Doppler Spectrum and Power Delay Profile

- **Re-interpretation of Doppler spectrum**

$$\boxed{\mathcal{S}(\nu) = \int \mathcal{C}_S(\nu, \tau)\, d\tau}$$

- **Power Delay Profile (PDP)**
  - Consider a WSSUS channel and $\Delta t = 0$, the PDP is defined as

$$R_h(t, t+\Delta t, \tau, \tau+\Delta\tau)\big|_{\Delta t=0} \stackrel{\Delta}{=} \mathcal{P}(\tau)\delta(\Delta\tau)$$

$$\Rightarrow \mathcal{P}(\tau) = E\left\{ |h(t,\tau)|^2 \right\}$$

Ensemble average ≡ temporal average by ergodicity (implicitly assumed)

Delay-Spread

- **The channel delay-spread is defined from the PDP as**

$$\tau_{RMS} = \sqrt{\frac{\int_0^\infty (\tau - \tau_M)^2 \mathcal{P}(\tau)\, d\tau}{\int_0^\infty \mathcal{P}(\tau)\, d\tau}}$$

$$\tau_M = \frac{\int_0^\infty \tau \mathcal{P}(\tau)\, d\tau}{\int_0^\infty \mathcal{P}(\tau)\, d\tau}$$

Extension to Double-Directional Channels

- When using antenna arrays, the directional spreading matters at both Tx and Rx
- Time-variant DD channel impulse response

$$h\left(t,\tau,\mathbf{\Omega}_t,\mathbf{\Omega}_r\right)=\sum_{k=0}^{n_s(t)-1} h_k\left(t,\tau,\mathbf{\Omega}_t,\mathbf{\Omega}_r\right)$$

  - n_s is the number of contributions
  - t and τ are the time and delay variables (same as non directional channels)
  - $\mathbf{\Omega}_t$ and $\mathbf{\Omega}_r$ are the Tx and Rx directions (DoD and DoA) in 3-D

Double Directional Correlation Functions

- Extension of Bello functions to the spatial/angular domains

[Oestges, 2007]

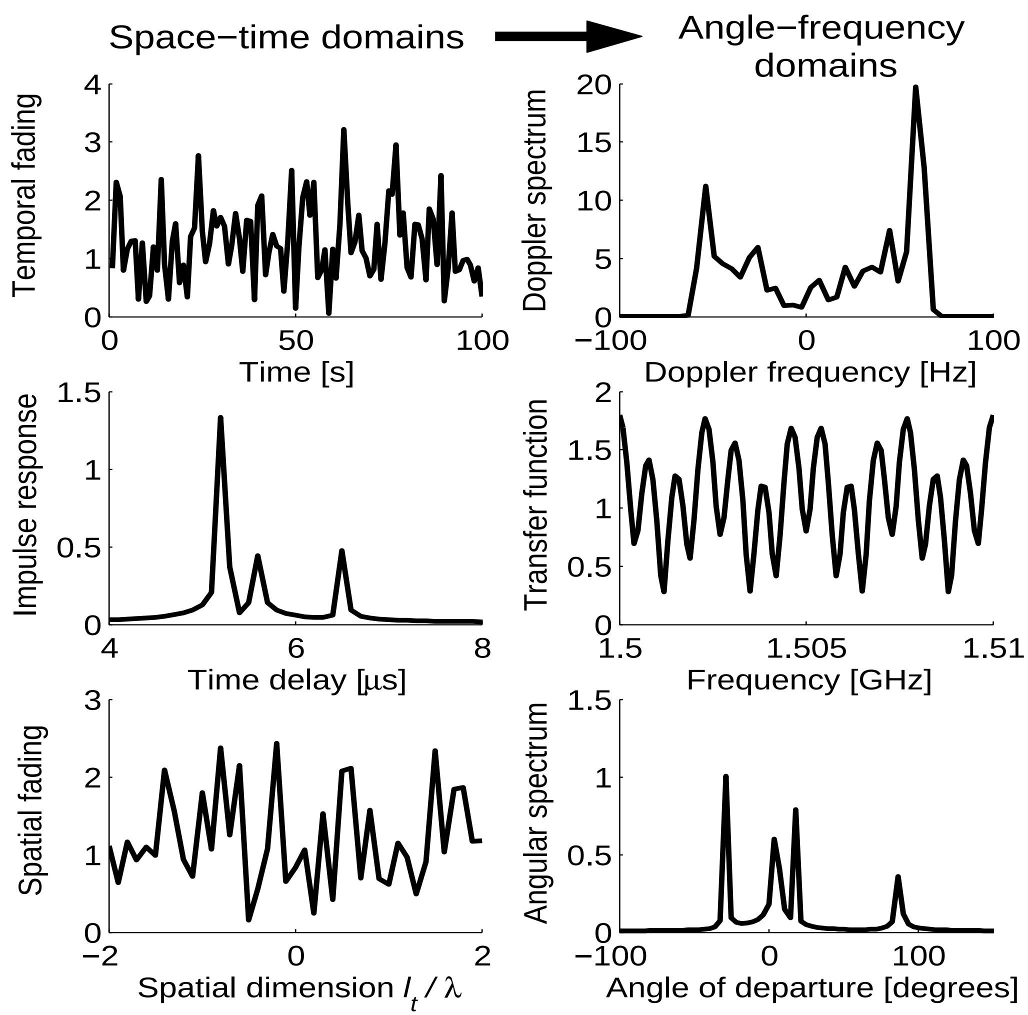

WSSUS-H Channels

- **WSS-US assumption**
  - Time and frequency correlations only depend on the time/frequency difference ⇔ signals arriving with different Doppler frequencies/delays are uncorrelated
- **Homogeneous assumption**
  - Spatial correlation only depends on the spatial difference at both Tx and Rx ⇔ signals departing/arriving with different directions are uncorrelated
  - True for linear arrays … not for arbitrary arrays

$$\boxed{R_S(\nu, \nu', \tau, \tau', \mathbf{\Omega}_t, \mathbf{\Omega}_t', \mathbf{\Omega}_r, \mathbf{\Omega}_r') = \mathcal{C}_S(\nu, \tau, \mathbf{\Omega}_t, \mathbf{\Omega}_r)\delta(\Delta\nu)\delta(\Delta\tau)\delta(\Delta\mathbf{\Omega}_t)\delta(\Delta\mathbf{\Omega}_r)}$$

Direction Power Spectra

- Joint, transmit and receive direction power spectra

$$
\begin{aligned}
\mathcal{A}(\mathbf{\Omega}_t, \mathbf{\Omega}_r) &= \mathcal{E}\left\{\left| \int h(t, \tau, \mathbf{\Omega}_t, \mathbf{\Omega}_r)\, d\tau \right|^2\right\} \\
&= \int \mathcal{P}_h(\tau, \mathbf{\Omega}_t, \mathbf{\Omega}_r)\, d\tau, \\
\mathcal{A}_t(\mathbf{\Omega}_t) &= \mathcal{E}\left\{\left| \iint h(t, \tau, \mathbf{\Omega}_t, \mathbf{\Omega}_r)\, d\tau\, d\mathbf{\Omega}_r \right|^2\right\} \\
&= \int\int \mathcal{P}_h(\tau, \mathbf{\Omega}_t, \mathbf{\Omega}_r)\, d\tau\, d\mathbf{\Omega}_r, \\
\mathcal{A}_r(\mathbf{\Omega}_r) &= \mathcal{E}\left\{\left| \iint h(t, \tau, \mathbf{\Omega}_t, \mathbf{\Omega}_r)\, d\tau\, d\mathbf{\Omega}_t \right|^2\right\} \\
&= \int\int \mathcal{P}_h(\tau, \mathbf{\Omega}_t, \mathbf{\Omega}_r)\, d\tau\, d\mathbf{\Omega}_t,
\end{aligned}
$$

Angular Spread

- **The channel angle-spreads are defined similarly to the delay-spread**

$$\boldsymbol{\Omega}_{t,M} = \frac{\int \boldsymbol{\Omega}_t \mathcal{A}_t(\boldsymbol{\Omega}_t)\, d\boldsymbol{\Omega}_t}{\int \mathcal{A}_t(\boldsymbol{\Omega}_t)\, d\boldsymbol{\Omega}_t}$$

$$\Omega_{t,RMS} = \sqrt{\frac{\int \left\|\boldsymbol{\Omega}_t - \boldsymbol{\Omega}_{t,M}\right\|^2 \mathcal{A}_t(\boldsymbol{\Omega}_t)\, d\boldsymbol{\Omega}_t}{\int \mathcal{A}_t(\boldsymbol{\Omega}_t)\, d\boldsymbol{\Omega}_t}}$$

UWB Channels

- **UWB systems** [Allen, 2006]
  - UWB is an extreme case of frequency-selective channels
  - UWB channels are also represented by taps in the delay domain
    - Because the bandwidth is large, each tap becomes more Ricean than Rayleigh
  - UWB models must however also account for the antenna distortion
    - The antenna becomes frequency-selective too !

Modeling Methods

- **Physical (deterministic) models**
  - Ray-tracing
  - Electromagnetic simulation tools
- **Empirical models**
  - Derive model parameters from measurements
    - Path loss models
    - Tapped delay line models
    - Standard models
    - Directional models

Ray-Tracing Techniques

- **Model features** [Oestges, 2007]
  - Buildings are represented by blocks with given material characteristics
  - Path-loss, shadowing and multipath fading are implicitly modelled all together
  - Geometrical optics: each mechanism is ray-modelled using Fresnel theory and Uniform Theory of Diffraction

$$h\left(\omega, \mathbf{T} \xrightarrow{\mathbf{Q}_m} \mathbf{R}\right) = \sum_m F_m(s,s')e^{-jks'} \cdot \mathbf{g}_m^{R^*} \cdot \mathbf{Q}_m \cdot \mathbf{g}_m^E \, K_m(s,s')e^{-jks} + \ldots$$

antenna gain and polarisation

complex dyadic coefficient

spreading factor

Ray-Tracing Techniques (2)

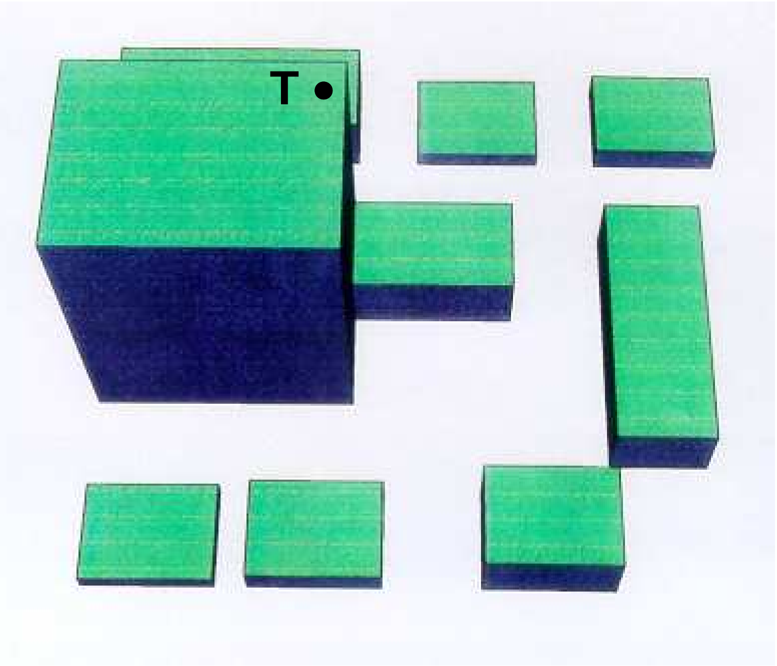

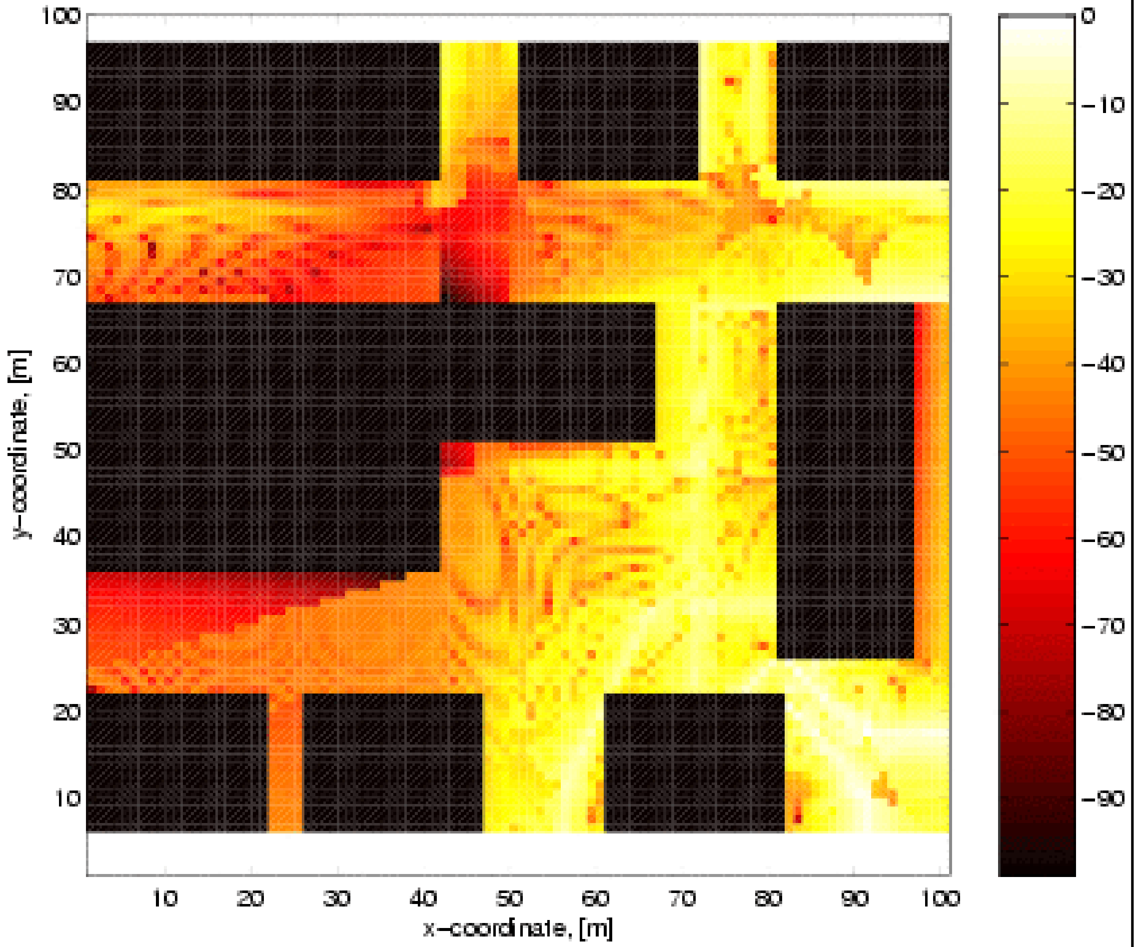

Tap Delay Line Models

- **Principle** [Saunders, 1999]
  - Express the channel IR as the sum of a number of independent taps, representing aggregated (filtered) multipaths
  - Each tap is a narrowband fading channel, with its delay, average power and statistics

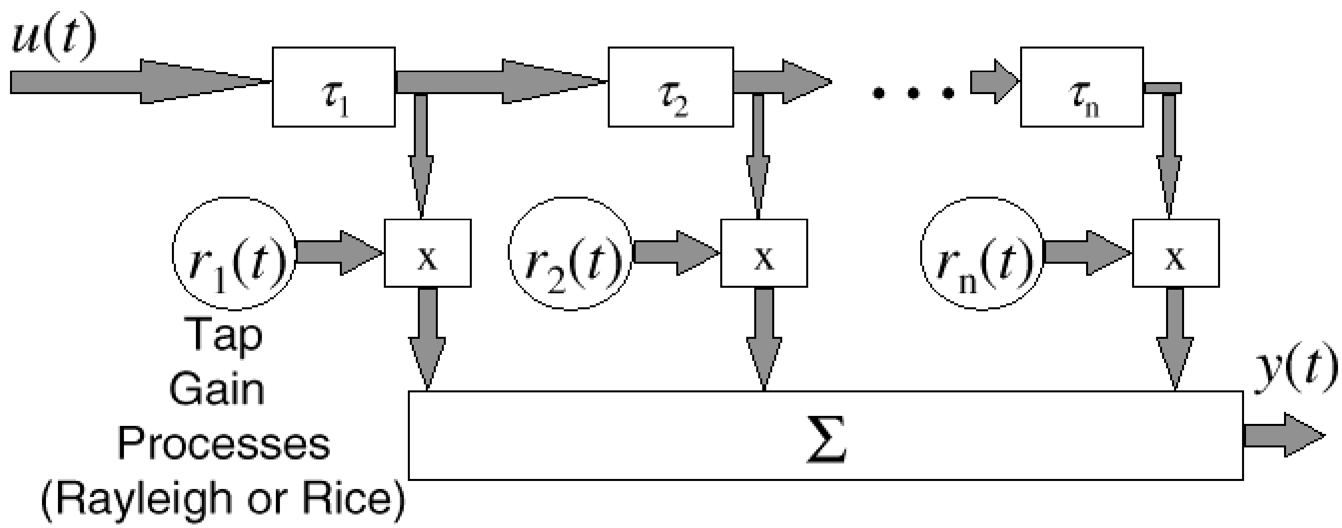

Standard Models

- **Example**
  - IEEE 802.15.4a for UWB Body Area Networks [Molish, 2006]
    - Saleh-Valenzuela model including tap correlations
      - Path-loss model
      - Macro- and microscopic scales
      - Power of macroscopic taps follows an exponential decay with delay
      - These taps are furthermore correlated (between themselves) !
    - More details later !

Directional Models

- **Modeling the directional spectrum**
  - Directional models are geometry-based

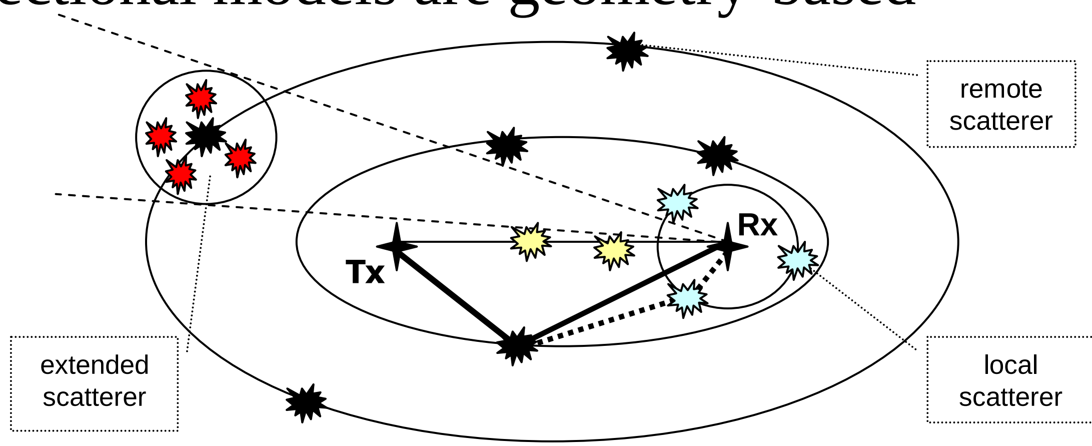

  - Models such as the WINNER, 3GPP or COST2100 model allow to take into account the directional dispersion [Oestges, 2007; Molisch, 2005]
  - However, these models are cellular MIMO-oriented, and not necessarily fitted to WSNs

Part II
Propagation for Wireless Sensor Networks

Particularities, Issues, Models

Propagation Medium

- **A large variety of scenarios**

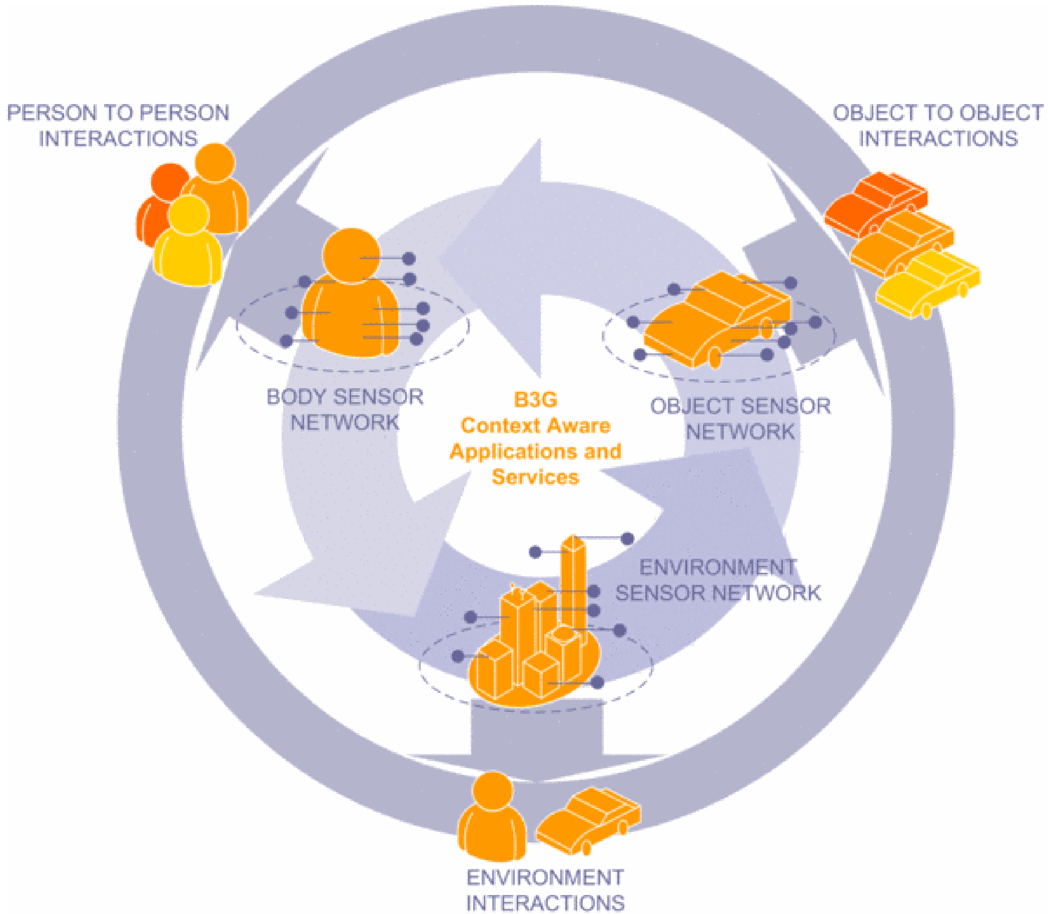

Propagation Medium

- **A large variety of scenarios**
  - WSNs are deployed in environments quite different from those usually modelled for cellular networks
  - A few examples
    - Body area networks
      - Sensing nodes are located on the body, or within clothes (wearable antennas)
    - Environmental WSNs
      - In this case, nodes can be distributed in a river, over the ground in a forest (this is quite different from a GSM user in a forest), etc.
      - Antenna heights are sensibly lower than in cellular systems
      - Electromagnetic characteristics of medium can be different
    - Industrial and automotive WSNs (car-to-car, in-car, etc.)
      - Antenna heights can be sensibly different
      - Proximity of metallic structures

Multi-Sensor Aspects

- **Virtual MIMO**
  - **Cooperative or relay schemes** can be thought of as virtual MIMO systems, where sensors communicate with central device via the creation of a virtual array or via relaying multi-hops
    - Relaying can solve range/SNR problems (e.g. body area networks)
    - Shadowing correlation is a critical parameter when estimating the performance

- **Relaying techniques**
  - Amplify and Forward (AF)
  - Decode and Forward (DF)

Multi-Sensor Aspects (2)

- **Channel models for multi-sensor networks**
  - Most signal processing techniques have been developed
    - For i.i.d. Rayleigh channels
    - Possibly with path-loss accounted for (SNR on each link depends on the Tx-Rx distance)
    - Often without shadowing and/or shadowing correlation
  - However in real-world
    - Shadowing is present and may be a correlated variable (impact on network ?)
    - Shadowing and fact fading cannot always be easily separated
    - Non coherent small-scale fading is often uncorrelated on different links, but what about the coherent contributions (LOS, fixed sensors, creeping waves) ?

AF Relay Channel

- Relay channel is made of two successive channels
  - Two-hop model

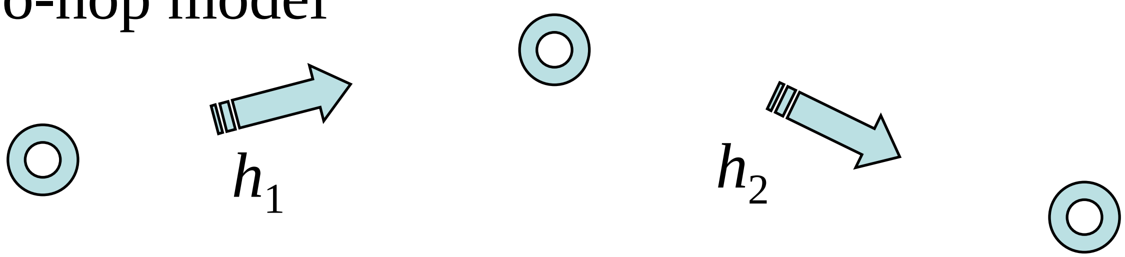

$$y = h_2 A \left[h_1 \sqrt{E_s}\, c + n_1 \right] + n_2$$

  - Global channel is the multiplication of Tx-Relay and Relay-Rx channels, with amplification factor *A*
    - h_1 and h_2 are Rayleigh fading channels with energy $2\sigma_1^2$ and $2\sigma_2^2$
    - n_1 and n_2 are noise contributions of power N
    - P_1 and P_2 are the transmit powers of nodes 1 and 2

AF Relay Channel (2)

- Amplification factor [Patel, 2006]
  - Fixed gain (depends on the CDIT of h_1)

$$A = \sqrt{\frac{P_2}{2P_1\sigma_1^2 + N}}$$

  - Variable gain (depends on the CSIT of h_1)

$$A = \sqrt{\frac{P_2}{P_1|h_1|^2 + N}}$$

AF Relay Channel Statistics (1)

- Overall relay channel is expressed as $h_{AF} = h_1 A h_2$
- For fixed relay gain (A arbitrarily fixed to 1) channels
  - Envelope PDF ($s = |h|$) for independent fading [Patel, 2006]

$$p_s(s) = \frac{s}{\sigma_1^2 \sigma_2^2} K_0 \left[\sqrt{\frac{s^2}{\sigma_1^2 \sigma_2^2}} \right]$$

  - Time correlation [Patel, 2006]
    - Will depend on the motion of all three nodes
    - For a FS-MS-MS link (assuming same frequency for both links)

$$R_h(\Delta t) = \left[J_0\left(\frac{2\pi}{\lambda} v_1 \, \Delta t \right) \right]^2 \cdot J_0\left(\frac{2\pi}{\lambda} v_2 \, \Delta t \right)$$

AF Relay Channel Statistics (2)

- Overall relay channel is expressed as $h_{AF} = h_1 A h_2$
- For fixed relay gain (A arbitrarily fixed to 1) channels
  - Envelope PDF for fully correlated fading

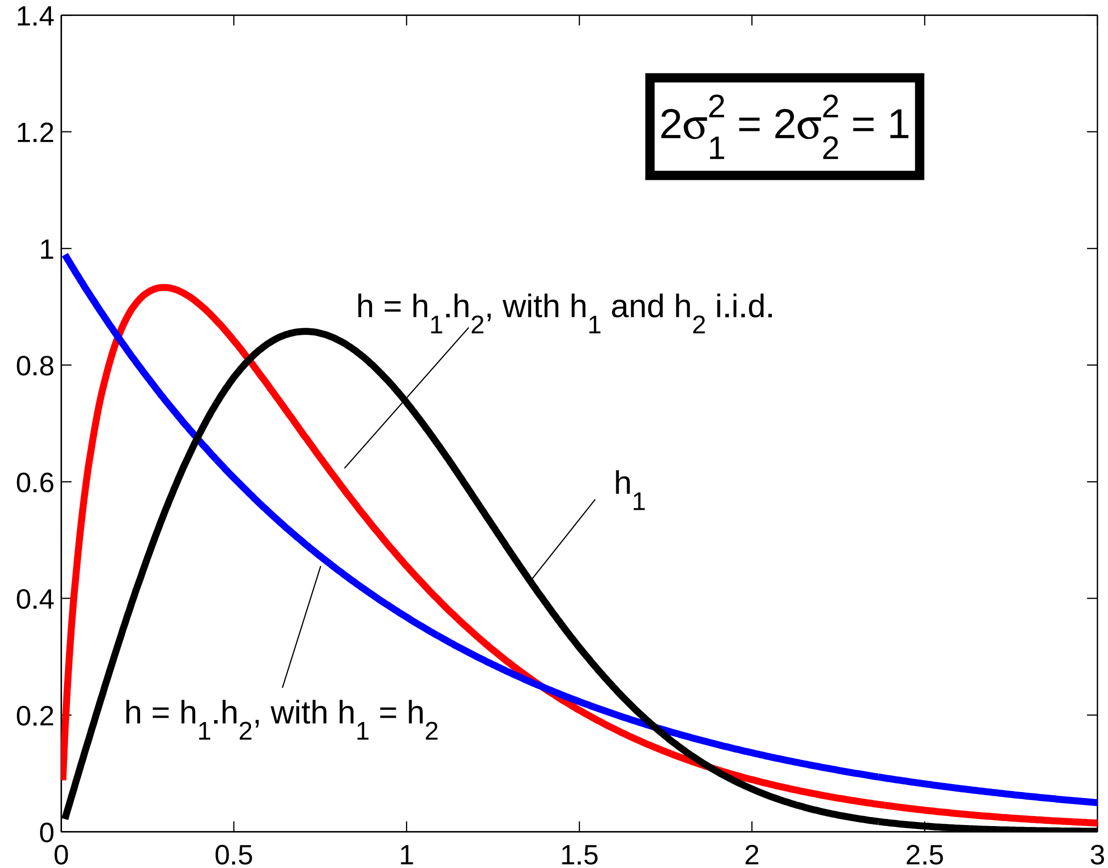

DF Relay Channel

- The relay decodes and re-encodes the information
  - Two successive links, with decode-encode process in-between
  - Overall channel cannot be expressed easily (of course !)

Part III
Example A: Environmental Sensor Networks

Environmental WSNs

- **Test case**
  - Wireless sensor networks in forest in the 2 GHz
  - Applications
    - Environmental sensors
    - Near-ground battlefield sensors
  - Low antenna height at both Tx and Rx (~ 0.3 ... 1.8 m)
  - Short range (~ 10 … 500 m)

Forest Channel Models

- **Path-loss *L* or excess attenuation *A***
  - h_m = 0.75m [Joshi, 2005]

$$L\,(dB) = -86.5 + 95.4\log_{10} d\,(m)$$

  - Modified ITU-R Rec. 833-4, h_m = 1.6m [Oestges, 2008]

$$A\,(dB) = 28\left[1 - \exp\left(-0.4d\,(m)\,/28\right)\right]$$

  - Lognormal shadowing of ~ 2.3 dB
  - Wet foliage
    - ~ 30 dB additional loss
  - Impact of antenna height
    - 4-5 dB path-loss decrease going from 0.75 to 1.6 m high

Forest Channel Models (2)

- **Fading**
  - Fixed sensors ⇒ fading is Ricean distributed (with d_0 = 100 m)

$$\boxed{K\,[dB] \approx 10 - 39\log_{10}(d/d_0)}$$

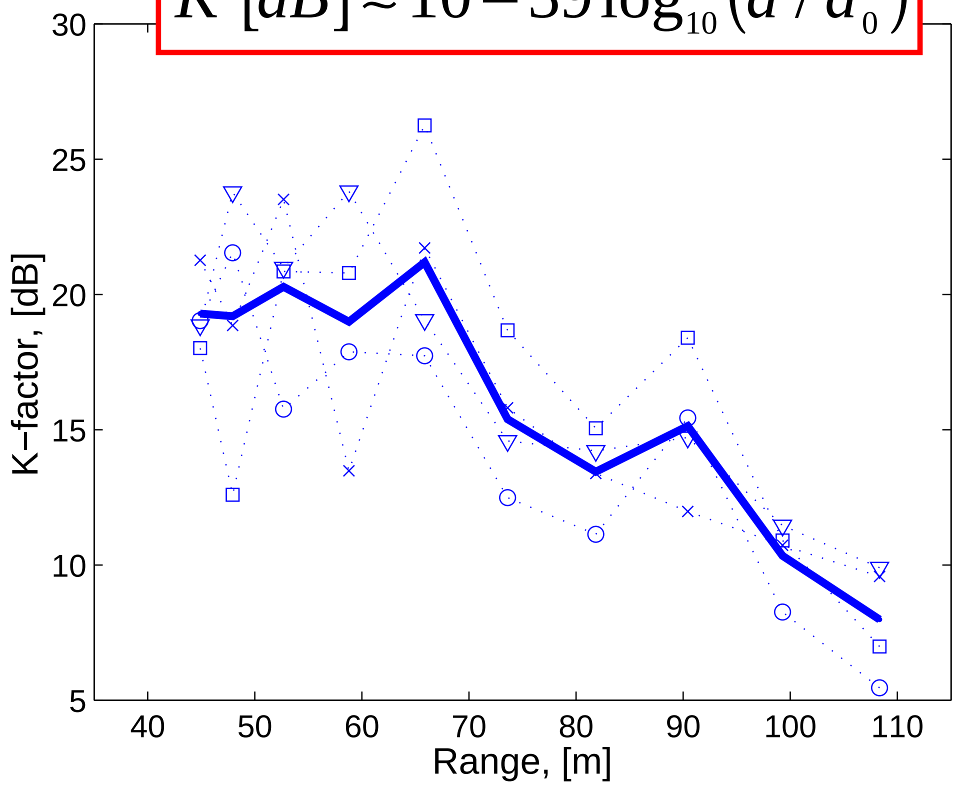

Forest Channel Models (3)

- **Delay-spread**
  - DS is much larger than for slant paths !
  - DS values range from 20 ns at d = 50 m up to 100 ns for d = 400 m for directional antennas, and are doubled for omnidirectional antennas [Joshi, 2005]
  - DS values range from 50 ns (d = 40 m) up to 120 ns (d = 120 m) for omnidirectional antennas [Oestges, 2008]
  - Impact of antenna height unclear
  -

Forest Channel Models (3)

- **Delay-spread**
  - DS is much lar
  - DS values rang
    d = 400 m for
    omnidirectiona
  - DS values rang
    120 m) for omı
  - Impact of anteı
  - –

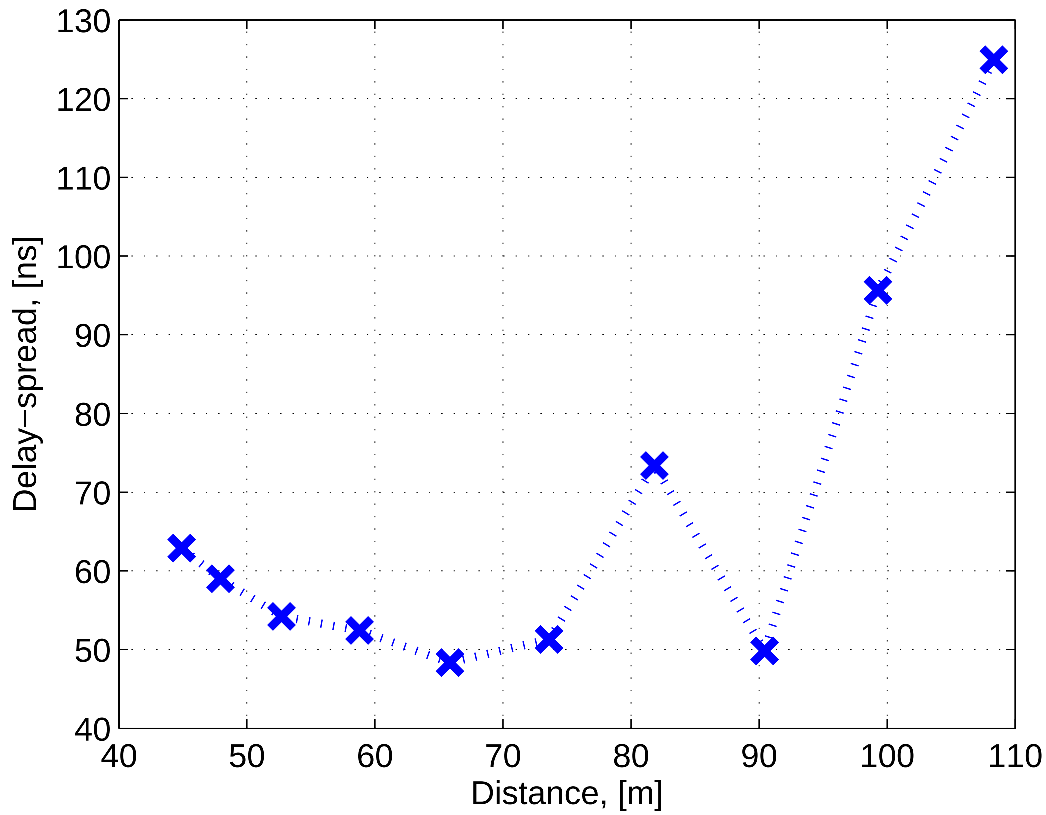

Forest Channel Models (4)

- **Angular dispersion**

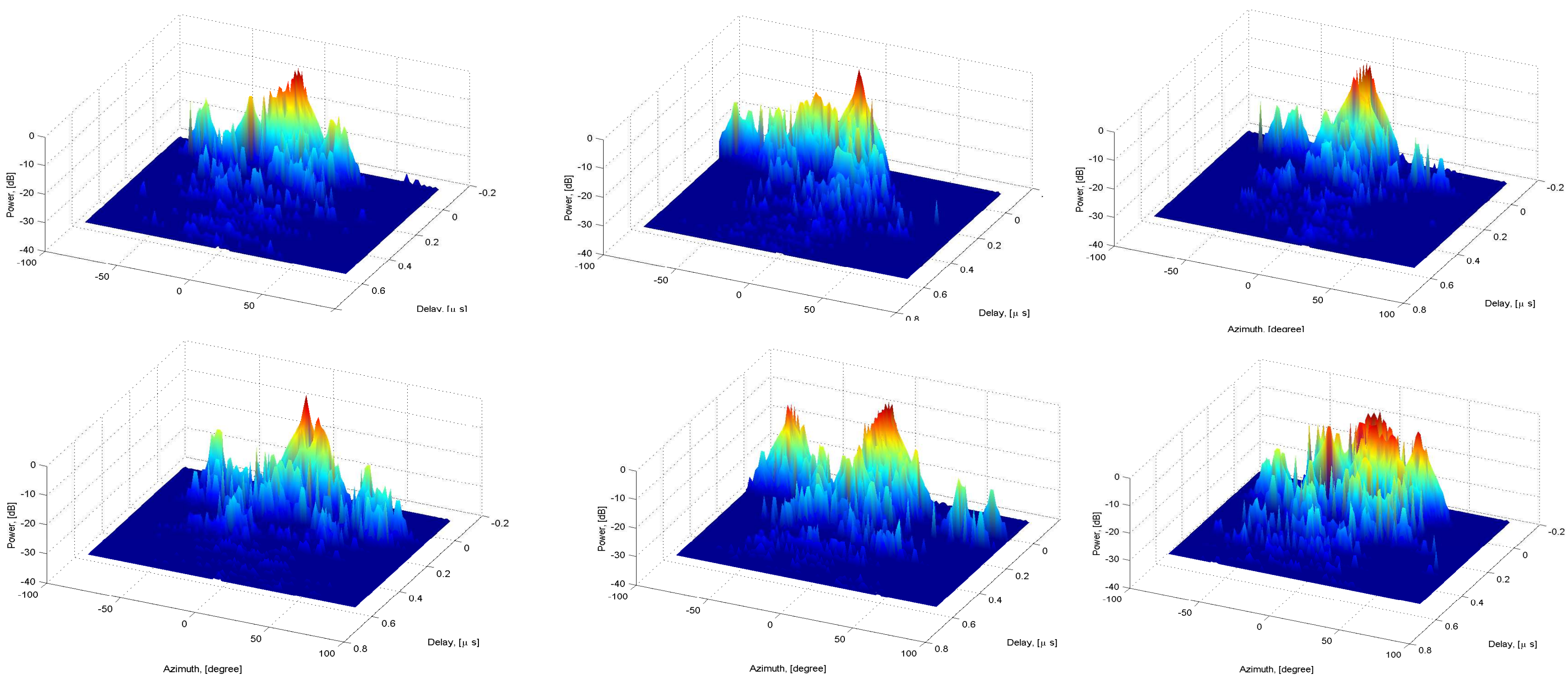

Forest Channel Models (5)

- **Shadowing correlation**
  - No experimental result so far …
  - Assumption
    - For aligned links, shadowing correlation is related to the distance difference

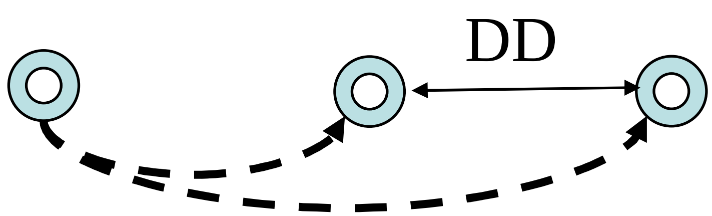

$$\rho \propto \exp\left(-\Delta D / \delta\right)$$

    - For non-aligned links, shadowing correlation is related to the angle difference

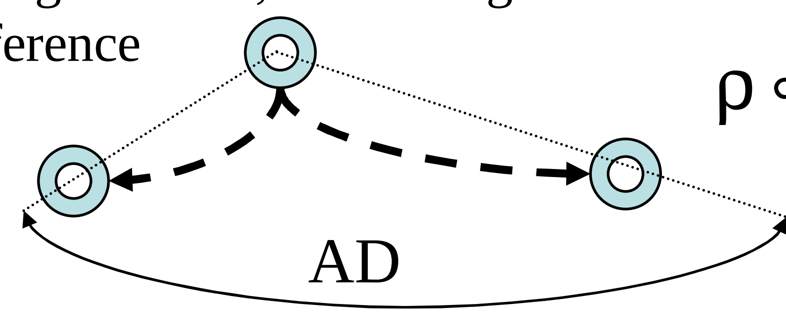

$$\rho \propto \exp\left(-\Delta \phi / \alpha\right)$$

Part III
Example B: Body Area Networks

Body Area Networks

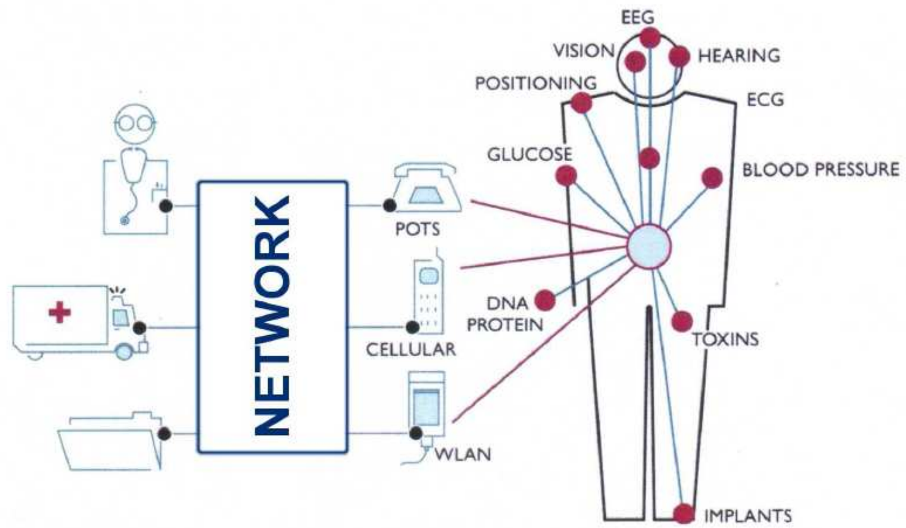

© IMEC

- Wireless sensors are distributed on the body or in clothes
  - EEG, ECG, EMG
  - Vision, hearing, etc.
  - Speed, etc.
- Central monitoring device (on- or off-body)
- Possible wireless link with larger network

Body Area Transmissions

- Various types of transmissions
  - Specific propagation mechanisms involved
  - Different models needed

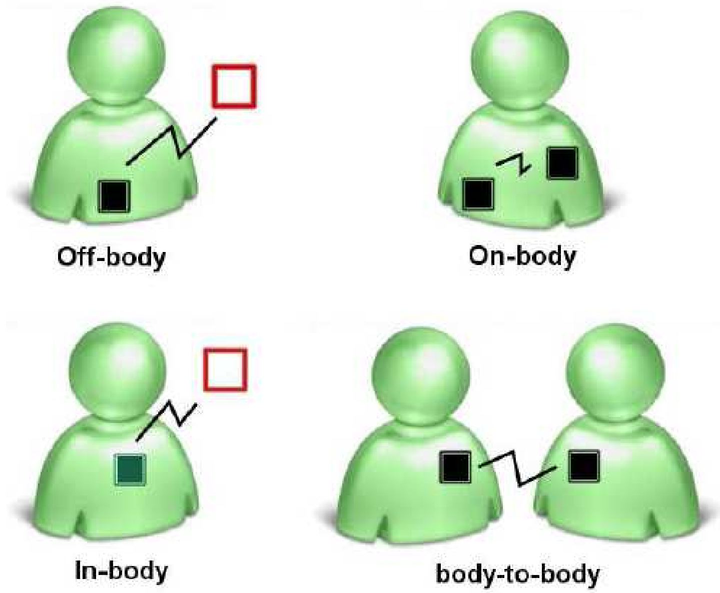

- Which technology ?
  - Narrowband (ZigBee, BT) ?
  - UWB ?

Body Area Propagation

- In-body penetration
- On-body propagation
- Off-body propagation
  - Arm reflection
  - Reflection/diffraction by external obstacles

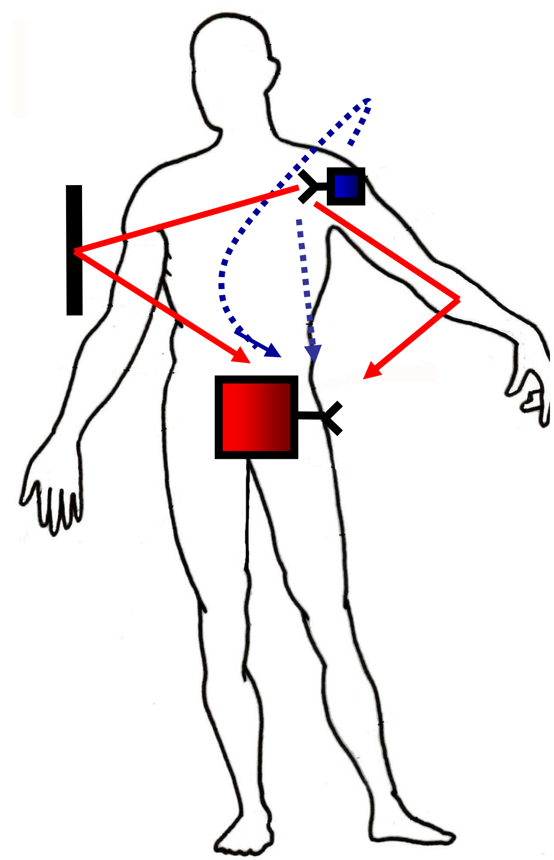

In-Body Penetration

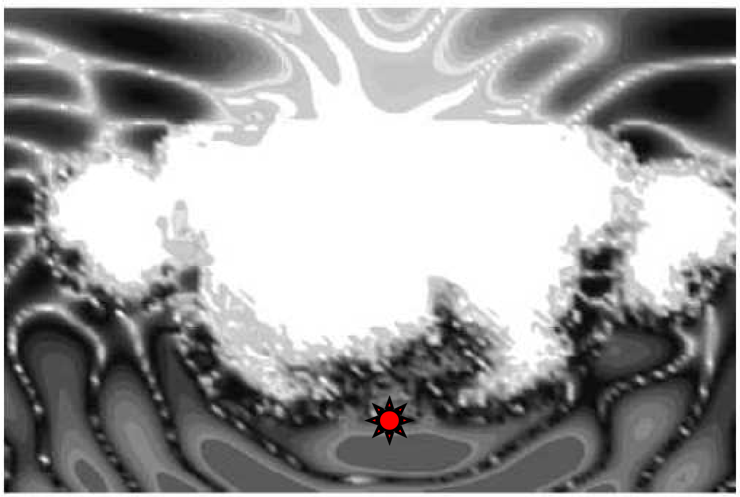

FDTD simulation

- Penetration decreases exponentially with frequency [Ryckaert, 2004]

$$L(dB) = \beta(r - r_0)$$

  – ~ 3 dB/cm at 400 MHz
  – ~ 4 dB/cm at 900 MHz
  – ~ 6 dB/cm at 2450 MHz

Front On-Body Propagation

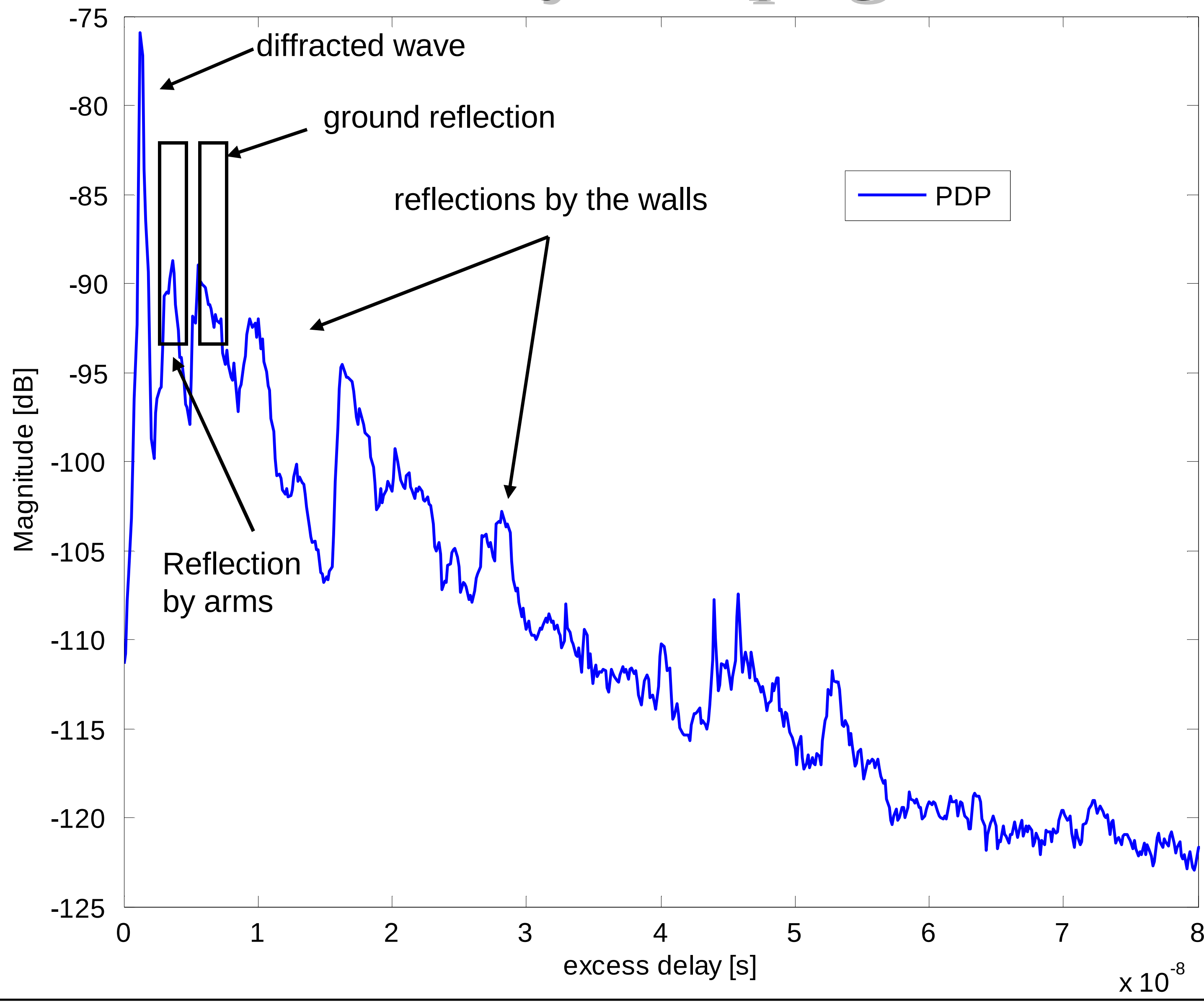

Front-to-Back On-Body Propagation

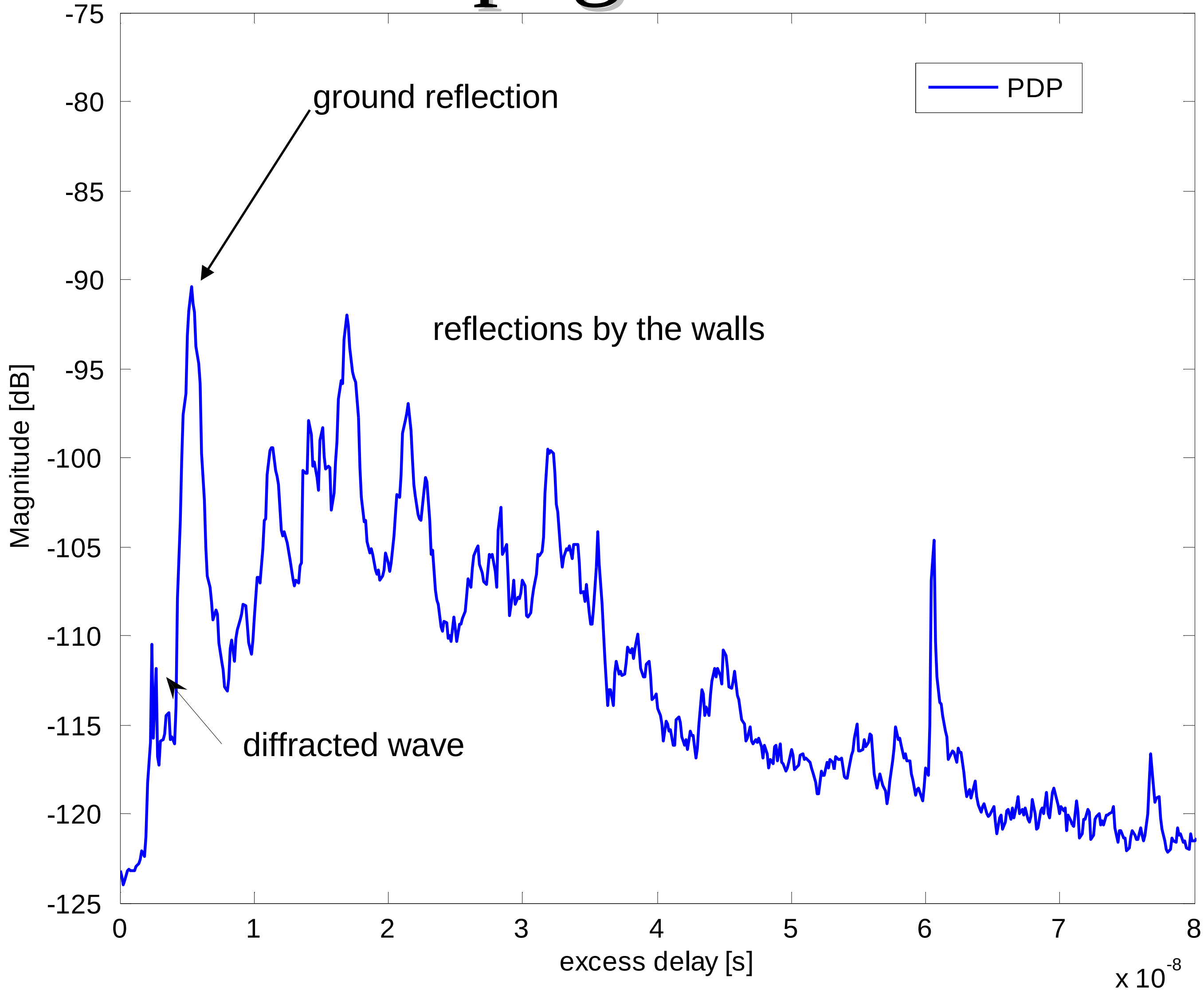

On- vs. Off-Body

- Received power from on- and off-body contributions
  - Simulations made for total energy in the 3-10 GHz band

	Diffracted wave [dB]	**Reflections [dB]**	**Total [dB]**	**Ratio body/total [%]**
F2F	-72.96	-70.28	-68.40	35.18
F2B	-100.70	-78.46	-78.43	0.60

  - Transmission from front to back hardly possible without scattering obstacles
  - Need of relaying strategy ?

On-Body Propagation

- **Existence of a diffracted wave a.k.a. body wave**
  - Diffracted wave is a creeping wave

    [Fort, 2008]

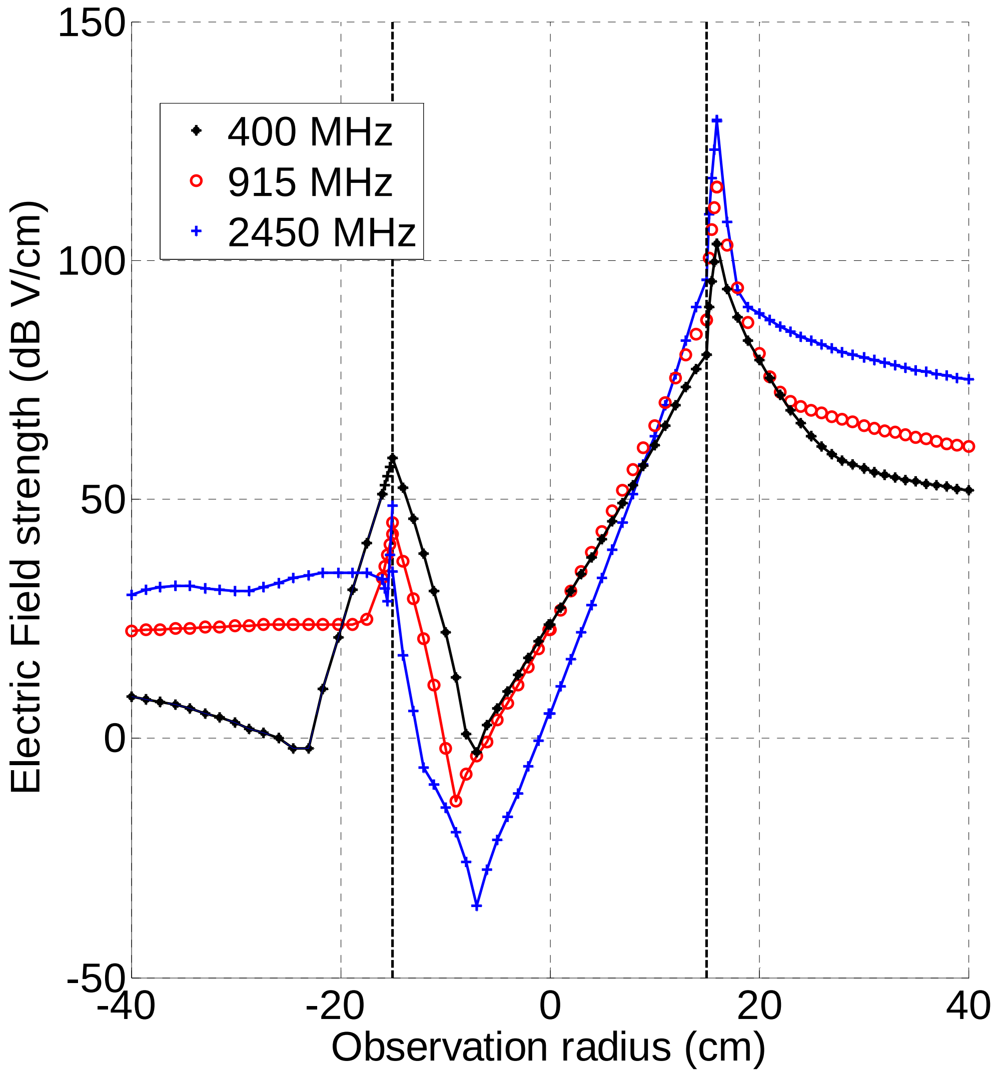

Propagation Velocity

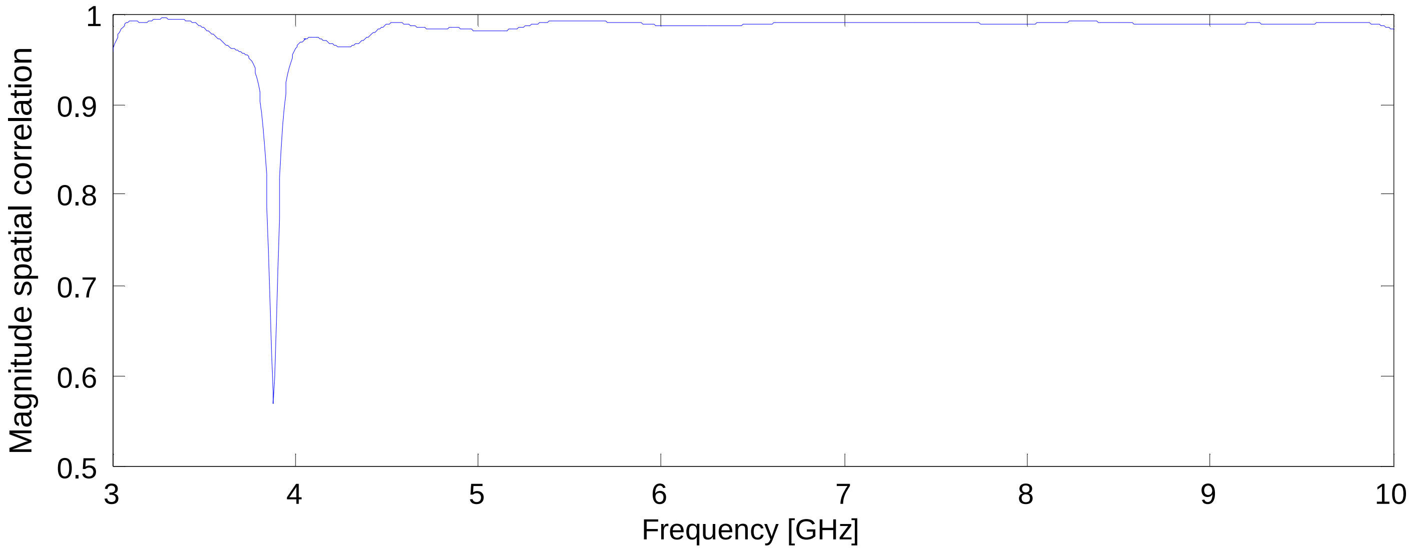

endfire

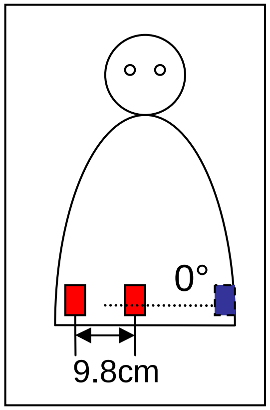

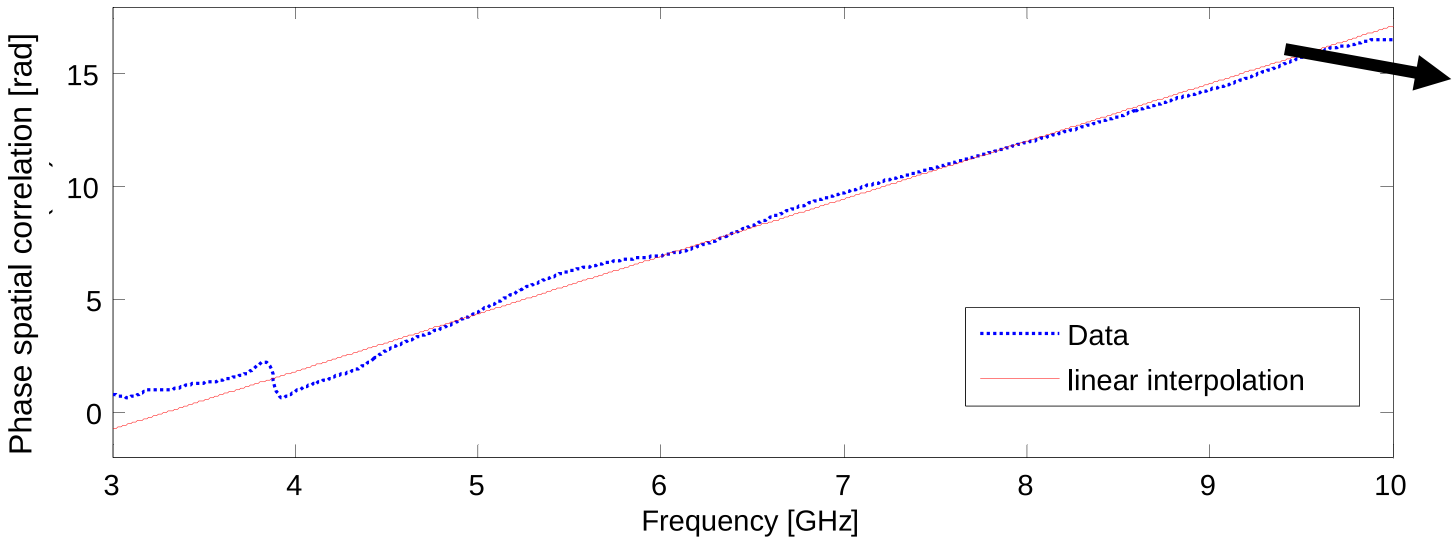

Linear phase

$$\Delta\varphi = \frac{2\pi}{\lambda} d \cos\theta$$

$$= \frac{2\pi}{\upsilon_{\varphi}} d \cos\theta \, f$$

Propagation Velocity (2)

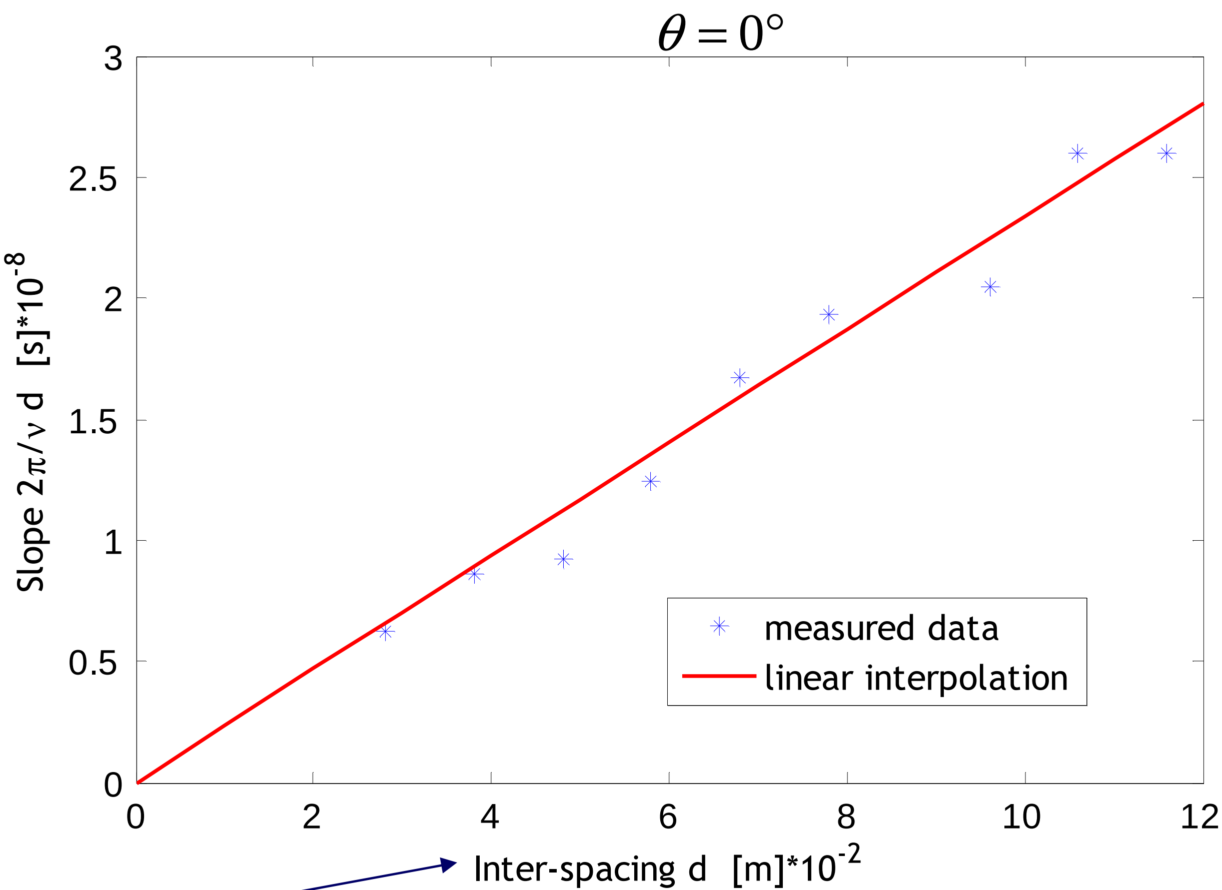

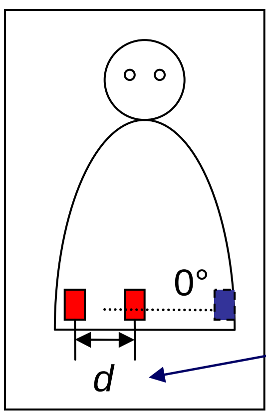

$\rightarrow \nu_\varphi = 2.66\ 10^8$ m/s [Van Roy, 2007]

On-Body Propagation (2)

- **Diffracted wave**
  - Attenuation can be very large
  - Along the body (same side)

$$L(dB) = 10m \log_{10}(r/r_0)$$

  - 30-35 dB/decade (m = 3 to 3.5 in the 900-2500 MHz frequency range)

$\Rightarrow$ ~ 25 dB between neck and waist at 2.45 GHz

On-Body Propagation (3)

- **Diffracted wave**
  - Around the body
    - Path-loss is exponential for small distances

$$L(dB) = \alpha(r - r_0)$$

    - Saturation in the back (for front Tx) caused by interference between right and left waves
    - Path loss is very high (2 dB/cm at 2.45 GHz)

$\Rightarrow$ ~ 40-50 dB from front to back

Off-Body Propagation

- **Impact of external environment**
  - External obstacles may create multipaths
  - They also help in providing a link when body wave is too much attenuated
    - That means that the transmission is heavily dependent on unreliable multipaths (in terms of occurrence, variability, etc.)

UWB Channel Model

- **Pathloss** (large-scale fading)

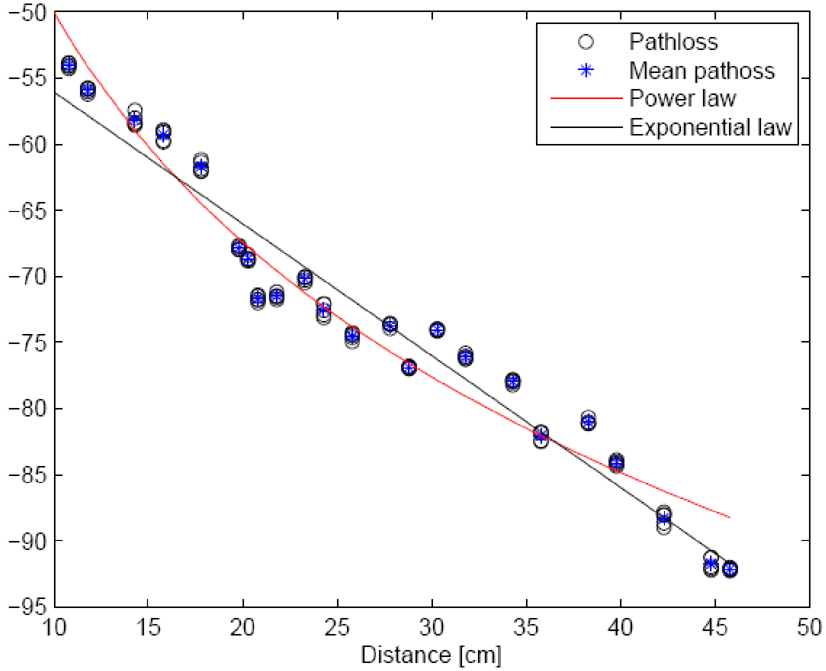

$$P_{(dB)}(d) = P_{(dB)}(d_0) - 10\ n\ \log_{10}\frac{d}{d_0}$$

$$P_{(dB)}(d) = P_{(dB)}(d_0) - \gamma\ (d - d_0)$$

	Loi classique		Loi exponentielle	
	$P_{(dB)}(d_0)$	n	$P_{(dB)}(d_0)$	γ [dB/cm]
3-10 GHz sans bras	-41.6	7.8	-49.4	1.3
3-10 GHz bras	-50.0	5.7	-56.0	1
3-6 GHz sans bras	-54.4	6.7	-61.5	1.1
3-6 GHz bras	-56.2	6.0	-62.6	1.0

Molisch		Fort	
d_0	10cm	d_0	10cm
$P_{(dB)}(d_0)$	-35.5dB	$P_{(dB)}(d_0)$	-50.5 dB
γ	1.078dB/cm	n	7.2

UWB Channel Model (2)

- **Tap-delay line model** [van Roy, 2008]
  - Lognormal distribution of tap amplitudes
  - Gaussian distribution in dB

$$\mathbf{A} = \mathbf{C}^{1/2}\mathbf{A}_w + \mathbf{M} + \mathbf{P}$$

N(0,1)

Normalized
tap average amplitude

Covariance matrix
(correlation is > 0.8
for adjacent taps

Path-loss

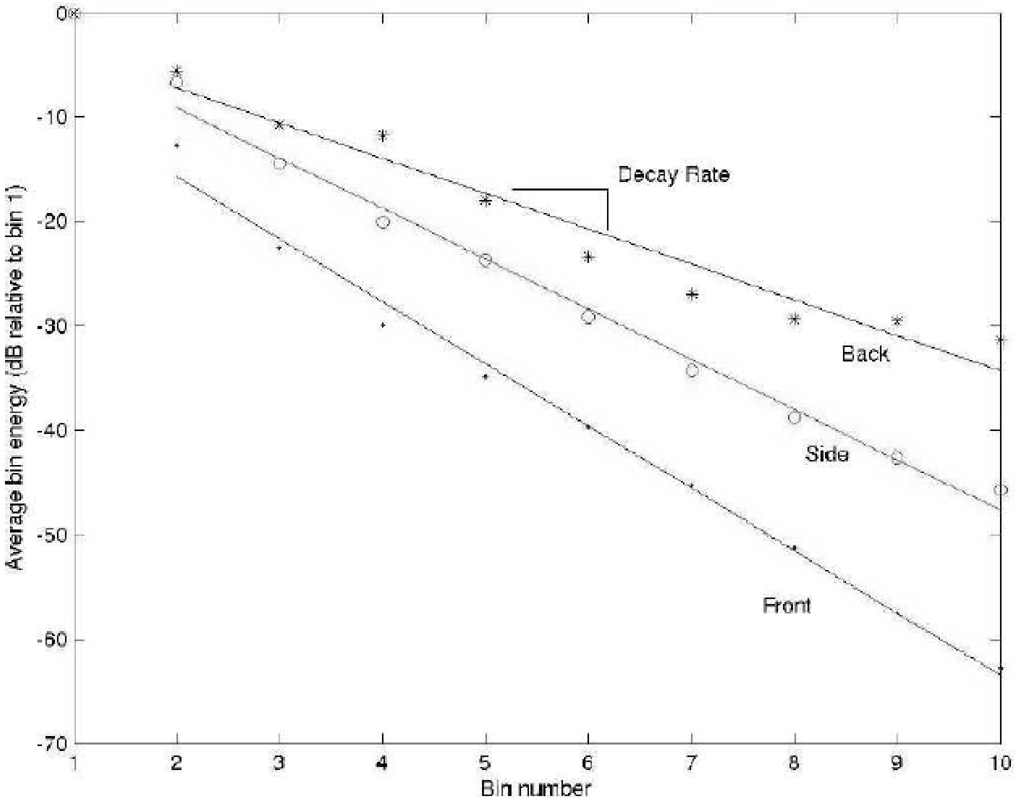

UWB Channel Model (3)

- Clustering of each tap: modified Saleh-Valenzuela model [Molisch, 2006; van Roy, 2008]

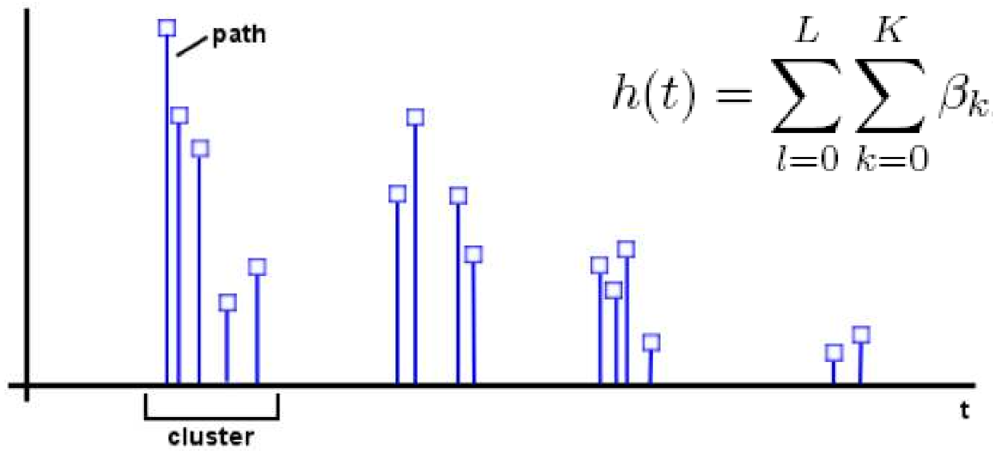

$$h(t) = \sum_{l=0}^{L} \sum_{k=0}^{K} \beta_{k,l} \delta(t - T_l - \tau_{k,l})$$

  - Cluster arrival time → Weibull distribution
  - Intra-cluster attenuation model → dual-slope model

Narrowband Cooperative Model

- Fading correlation between different channels
  - For aligned channels around the torso, shadowing correlation appear to lineraly decrease with the distance difference (DD)
  - Decorrelation DD is about 20 cm at 2.45 GHz [Liu, 2008]

References

B. Allen, M. Dohler, E. Okon, and W. Malik , *Ultra wideband antennas and propagation for communications, radar and imaging*, Wiley: New York, 2006.

A. Fort, J. Ryckaert, C. Desset, P. De Doncker, P. Wambacq, L. Van Biesen, Ultra-wideband channel Model for communication around the human body , *IEEE J. Sel. Areas Commun.*, vol. 24, no. 4, 2006.

A. Fort, G. Roqueta, C. Craeye, C. Oestges, A body area propagation model derived from fundamental principles: analytical analysis and comparison with measurements, *IEEE Trans. Ant. Propagat.*, accepted for publication.

A. Goldsmith, *Wireless communications*, Cambridge University Press: Cambridge, 2005.

G.G. Joshi, et al., "Near-ground channel measurements over line-of-sight and forested paths," *IEE Proc. Microwaves, Antennas and Propagation*, vol. 152, no. 6, pp. 589-596, 2005.

References (2)

L. Liu, P. De Doncker, C. Oestges, Fading correlation analysis for front abdomen propagation in body area networks, COST 2100 MCM 5 (Trondheim, Norway), TD(08) 522, 2008.

A.F. Molisch, *Wireless Communications*, Wiley: New York, 2005.

A.F. Molisch, D. Cassioli, C.-C. Chong, S. Emami, A. Fort, B. Kannan, J. Karedal, J. Kunisch, H.G. Schantz, K. Siwiak, and M.Z. Win, A comprehensive standardized model for ultrawideband propagation channels, *IEEE Trans. Antennas and Propag*., vol. 54, no. 11, pp. 3143-3150, 2006.

C. Oestges and B. Clerckx, *MIMO wireless communications: from real-word propagation to space-time code design*, Academic Press: Oxford, 2007.

C. Oestges, B. Montenegro-Villacieros and D. Vanhoenacker-Janvier, "Multi-dispersive channel characterization for radio localization-based rescue search," 3rd International Conference on Communications and Networking in China, Chinacom 2008 (Hangzhou, China), August 2008.

References (3)

C.S. Patel, G.L. Stüber, T.G. Pratt, Simulation of Rayleigh faded mobile-to-mobile communication channels, *IEEE Trans. Comm.*, vol. 53, no. 11, , pp. 1876-1884, 2005.

C.S. Patel, G.L. Stüber, T.G. Pratt, Statistical properties of amplify and forward relay fading channels, IEEE Trans. Veh. Techn., vol. 55, no. 1, , pp. 1-9, 2006.

J. Ryckaert, P. De Doncker, S. Donnay, A. Delehoye, R. Meys, Channel model for wireless communication around the human body, *Electronics Letters*, vol. 40, no. 9, pp. 543-544, 2004.

S. Saunders, *Antennas and propagation for wireless communication systems*, Wiley: Chichester, 1999.

S. van Roy, C. Oestges, F. Horlin, P. De Doncker, On-body propagation velocity estimation using ultra-wideband frequency-domain spatial correlation analyses, *Electronics Letters*, vol. 43, no. 25, pp. 1405-1406, December 2007.

S. van Roy, C. Oestges, F. Horlin, P. De Doncker, A spatially-correlated tapped delay line model for body area networks, 68th IEEE Vehicular Technology Conference Fall, VTC-Fall ‘08 (Calgary, AB), September 2008.